

A Genealogy of Multi-Sensor Foundation Models in Remote Sensing

KEVIN LANE and MORTEZA KARIMZADEH, University of Colorado, Boulder, USA

Foundation models have garnered increasing attention for representation learning in remote sensing, primarily adopting approaches that have demonstrated success in computer vision with minimal domain-specific modification. However, the development and application of foundation models in this field are still burgeoning, as there are a variety of competing approaches that each come with significant benefits and drawbacks. This paper examines these approaches along with their roots in the computer vision field in order to characterize potential advantages and pitfalls while outlining future directions to further improve remote sensing-specific foundation models. We discuss the quality of the learned representations and methods to alleviate the need for massive compute resources. We place emphasis on the multi-sensor aspect of Earth observations, and the extent to which existing approaches leverage multiple sensors in training foundation models in relation to multi-modal foundation models. Finally, we identify opportunities for further harnessing the vast amounts of unlabeled, seasonal, and multi-sensor remote sensing observations.

CCS Concepts: • **General and reference** → **Surveys and overviews**; • **Computing methodologies** → **Image representations**; **Reconstruction**; • **Applied computing** → **Environmental sciences**; • **Information systems** → **Spatial-temporal systems**.

Additional Key Words and Phrases: Foundation Models, Remote Sensing, Self-Supervised Learning

ACM Reference Format:

Kevin Lane and Morteza Karimzadeh. 2025. A Genealogy of Multi-Sensor Foundation Models in Remote Sensing. 1, 1 (April 2025), 26 pages. <https://doi.org/10.1145/nnnnnnnn.nnnnnnnn>

1 Introduction

With the recent successes of Natural Language Processing (NLP) frameworks like Generative Pre-trained Transformers (GPT) [69] and Bi-directional Encoder Representations from Transformers (BERT) [49], the development and application of machine learning is shifting away from focusing on transfer learning, which utilized traditional supervised learning on a large, labeled dataset to learn representations of that data to apply to other related tasks. Instead, Self-Supervised Learning (SSL), which attempts to learn general-purpose representations of data, known as encodings, has risen in popularity, showing considerable improvement in the quality of learned representations [16]. These models have a number of advantages over their predecessors, particularly in their ability to leverage vast amounts of unlabelled data. As datasets have grown larger, with some datasets now containing billions of datapoints [25], the process of labeling data for supervised learning has proven to be a costly bottleneck for improving model performance. Learning encodings through SSL has allowed researchers to fine-tune models for specific downstream tasks on significantly smaller labeled datasets in order to achieve state of the art (SOTA) performance on a single task. These generalizable representations can be utilized for any number of downstream tasks within a domain. Decoupling the process of learning encodings

Authors' Contact Information: Kevin Lane, kevin.lane@colorado.edu; Morteza Karimzadeh, karimzadeh@colorado.edu, University of Colorado, Boulder, Colorado, USA.

Permission to make digital or hard copies of all or part of this work for personal or classroom use is granted without fee provided that copies are not made or distributed for profit or commercial advantage and that copies bear this notice and the full citation on the first page. Copyrights for components of this work owned by others than the author(s) must be honored. Abstracting with credit is permitted. To copy otherwise, or republish, to post on servers or to redistribute to lists, requires prior specific permission and/or a fee. Request permissions from permissions@acm.org.

© 2025 Copyright held by the owner/author(s). Publication rights licensed to ACM.

Manuscript submitted to ACM

from the process of learning downstream tasks enables downstream users to leverage high performance machine learning models and minimizes the amount of labeled training samples needed to learn specific tasks.

In the wake of NLP success, the computer vision (CV) field swiftly delved into SSL with models such as BYOL [31], SimCLR [14], MoCo [34], and DINO [9], all of which use unique approaches to create self-supervised tasks and objectives for natural imagery data. These methodologies have recently started to percolate into the field of remote sensing (RS), where the sheer amount of unlabelled data from satellite imagery makes the field ripe for the development of foundation models. The importance of enabling training with fewer labeled samples for environmental monitoring in the face of climate change, such as monitoring or forecasting wildfires and flooding, means that there is imminent use for these generalized representations for downstream tasks. Thus far, the self-supervised methods for foundation models in RS build heavily upon CV methods and fall broadly into one of three categories:

- (1) Contrastive learning via negative sampling
- (2) Contrastive learning via distillation
- (3) Masked auto-encoding

Most of these approaches have demonstrated significant promise in the RS domain but have largely remained limited to applying the same CV frameworks to satellite imagery and other remote sensing datasets with few to no methodology changes [75]. On the other hand, recent research demonstrates how satellite data has unique properties that are distinct from natural imagery, such as the logarithmic distribution of objects and the range of the electromagnetic spectrum captured within satellite images [75]. These properties indicate that satellite imagery is a distinct modality and would therefore benefit from modality-specific frameworks and self-supervised learning tasks. Moreover, the variety of different satellite and ground-level sensors available allows for the development of highly specialized multi-modal foundation models.

Recent papers in the field have surveyed available foundation models in RS. Zhou explored the high potential of applied Vision Language Models (VLMS) while highlighting their few shot capabilities in downstream tasks [105]. Lu examined the model backbones used in foundation models, taking care to touch on ResNet [35] and Transformer [92] backbones, and compiled results for RS foundation models across a wide range of diverse downstream tasks [60]. Chen inspected how models can adapt to utilize non-raster based data [16], while Zhang examined the singular task of building foundation models specifically for urban environments [103], and Mai created a list of traits desirable in RS foundation models [62]. While these works provide a timely review of important components in RS foundation models, none of them focus on understanding the origins of RS SSL techniques and the modifications that have been developed for handling RS data, or those modifications that intend to alleviate the need for substantial computational resources. These modifications are critical to model performance and understanding them is necessary for the development of future multi-modal RS foundation models. In this paper, we contribute to the growing body of research on foundation models in remote sensing by doing the following:

- (1) We further demonstrate how the modes of data available in RS provide unique information that sets them apart from the natural imagery of CV.
- (2) We survey recent foundation models developed in the field, categorized by their learning objective, approach and compute requirements, and discuss their specific adaptations for RS observations.
- (3) We identify gaps, and lay out research opportunities for foundation models that specifically consider the multi-sensor and multi-modal nature of RS observations.

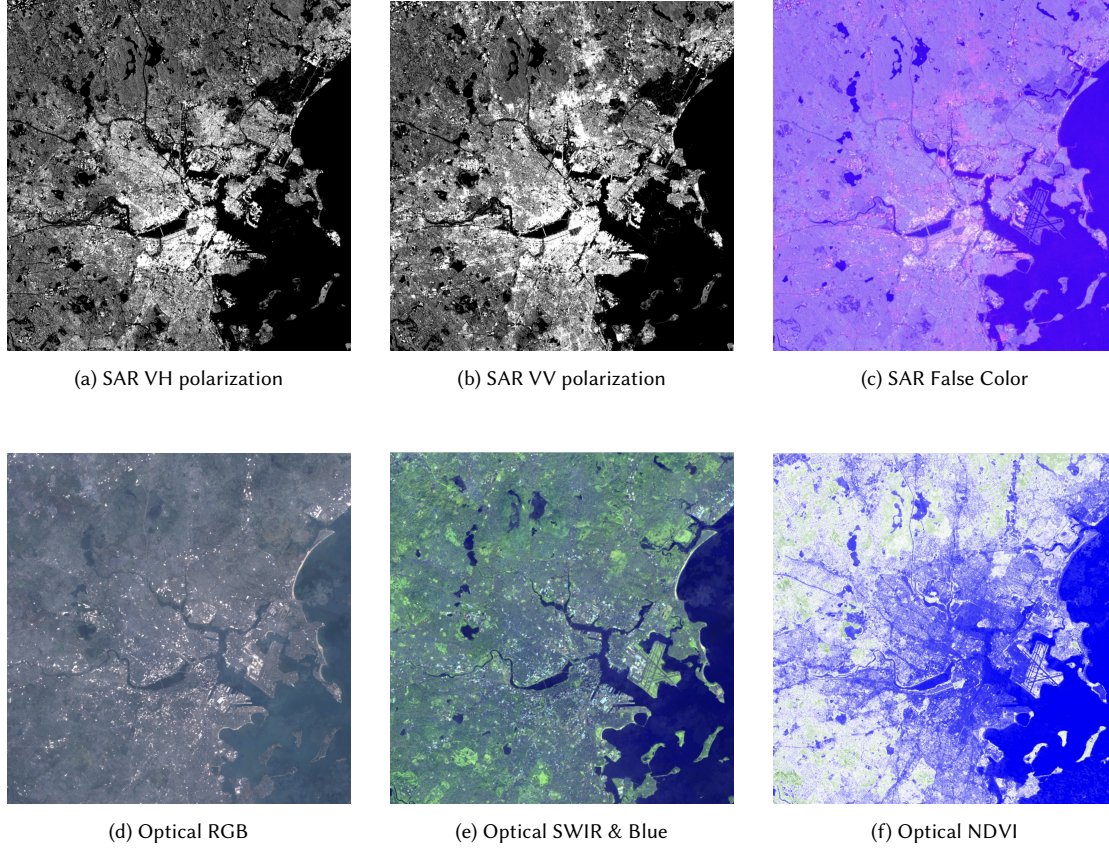


Fig. 1. Satellite imagery of Boston, MA in October, 2020. SAR imagery is obtained from Sentinel-1, and optical imagery is obtained from Sentinel-2. SAR false color uses VV polarization for red channel, VH polarization for green channel, and the average of VV and VH polarizations for blue channel. NDVI refers to the Normalized Difference Vegetation Index, an index based on the Red and NIR bands that is utilized to assess vegetation health.

2 Data for Training Remote Sensing Foundation Models

The CV field has primarily been concerned with natural images, which only sense the red, green, and blue wavelengths of the visible spectrum, and are typically captured at ground level. Some models, such as CLIP [73], FLIP [45], VisualBERT [52], ViLBERT [59], FLAVA [80], and DeepSeek-VL2 [98] are VLMs that also utilize text as an additional mode of data. However, most of the RS foundation model frameworks borrowed from CV concern themselves with only the image modality. Within the RS domain, the variety of unique sensors available ranges across a number of instruments aboard different satellites. The data modes detailed below are available at mass scale and readily accessible for training foundation models, which is our focus in this manuscript, rather than providing a full catalogue of remote sensing or geospatial data. We will keep discussions focused on sensors with high resolution (e.g., less than 40m), which are also the focus of current efforts in benchmarking datasets [51] and training foundation models [105].

2.1 Optical Imagery

Optical images capture electromagnetic wavelengths in the visible and near visible bands of light. These are recorded via passive sensors, which simply measure the electromagnetic radiation originating from the sun that is reflected off of objects. This means that passive sensors are more energy efficient than active sensors, but they are affected by light and weather conditions. These sensors can only capture imagery during the daytime, and can be obscured by atmospheric phenomena like cloud cover or haze, making their use limited in hurricanes, storms or active floods under overcast conditions.

Optical images are often acquired from different satellites, with several openly available freely for mass download, such as MODIS [47], the Landsat [99] family, and Sentinel-2 [83], with the latter two offering high resolution. Each satellite contains a sensor with different spatial and spectral resolutions, but each is broadly designed to capture the visible, near-infrared, and short-wave infrared portions of the electromagnetic spectrum. In the case of the Sentinel-2 satellite, there are 13 distinct bands that are captured at resolutions ranging from 10m/pixel to 60m/pixel, and can be broken down into five groups based on usage as follows [94]:

- B1 is the coastal aerosol band, useful for mapping coastal marine habitats and bathymetry. [71]
- B2-4 capture RGB (Red Green Blue), similar to digital cameras.
- B5-8 refer to VNIR (Visible and Near Infrared) light, and are typically used to measure vegetation health. B8a is a Narrow NIR band for moisture-based vegetation health monitoring.
- B9, still in NIR spectrum, focuses on water vapor absorption and is used to measure atmospheric moisture presence, and paired with B8A to derive total precipitable water.
- B10-B11 are SWIR (Short Wave Infrared) bands, with B10 for cirrus cloud detection, B11 for soil and vegetation moisture detection and snow/ice vs. cloud differentiation, and B12 is often used with B2 to measure geological features and mapping burned areas.

This range of spectrum and information captured by Sentinel-2 is an example of the wealth of information is captured by remote sensing optical products that go beyond RGB. However, CV models are designed to operate with three input channels of RGB of ‘natural’ images (obtained by regular cameras and widely available on the internet). In order to leverage the highly sophisticated pre-trained weights that are available for CV models such as the ubiquitous ResNet50 or ViT16, some RS models, such as SeCo [64] or MMCP [17], only utilize the visible bands of light from MS satellite images. RS models also rely on RGB images taken at ground level [11], or from some sort of aerial platform, such as a drone or helicopter [55]. While RS models trained purely on RGB can achieve SOTA performance in certain settings [64], deep learning models in RS that only train on RGB data have an information disadvantage compared to models that train on all bands and can struggle to perform on a number of downstream tasks in RS as a result [51]. The spectral range of interest and the specific choice of bands on a satellite are the result of decades of experience, in-lab experiments and consensus-building efforts to ensure satellites are equipped with bands that can assist in target-specific tasks. Figure 1 highlights the information lost when solely examining RGB imagery. For instance, infrared bands are crucial for monitoring vegetation [68], as seen in figure 1f, while NIR bands in confluence with blue and green bands can help with water quality analysis [20]. Shortwave infrared (SWIR) can be used for measuring soil and vegetation moisture, and is depicted in figure 1e.

While increasingly, foundation models leverage most bands present in optical imagery such as Sentinel-2, they typically do so by a simple manipulation of input channel dimensions to the image encoder of the model [95]. The optimal architecture required for remote sensing architectures is not well-defined yet [75].

2.2 Synthetic Aperture Radar

Synthetic Aperture Radar (SAR) is an active remote sensor that emits energy in microwave frequencies towards the earth and then captures the amount of energy reflected back. Capturing the image from a moving sensor (in this case, a satellite) allows for capturing the image through a large 'synthetic' aperture, compared to the much smaller physical sensor aperture, resulting in a much higher resolution than other sensors that monitor similar frequencies [7]. Each SAR sensor operates in a specific wavelength, referred to as bands, which serve different uses [91]. Larger wavelengths provide more penetration through obstruction, such as vegetation, but result in lower resolution. One of the most commonly used bands is the C-band (7.5-3.8 cm wavelength) [91], which is currently captured by Sentinel-1 [89], RADARSAT-1 [61], RADARSAT-2 [65], RADARSAT Constellation Mission (RCM) [88] satellites, and made available publicly, and is useful for global mapping and change detection, as its larger wavelength provides moderate penetration still at relatively high spatial resolution (e.g., 40m). However, there are larger wavelengths available, such as L-band, which is captured by AirSAR [37], PALSAR [77], and the soon-to-be-launched NISAR [12]. L-band is often used for biomass and vegetation mapping [32]. There is also X-band, whose wavelength is smaller than C-band and often used for high resolution monitoring of fine surface features, such as vegetation structure, and urban infrastructure. [82]. X-band is obtained by platforms such as Capella [10], ICEYE [40], TerraSAR-X [97], and TanDEM-X [50]. Different wavelengths of SAR capture different information, and different wavelengths often complement each other, if available for the same region and time.

SAR has another distinct characteristic from optical imagery: SAR takes advantage of materials' innate dielectric properties; every material has a dielectric constant that describes how strongly it interacts with electromagnetic waves. Materials with a high dielectric constant, such as water, reflects microwave energy back more strongly, allowing it to be picked up more easily by SAR [5]. This can prove useful for applications such as mapping waterways in a region that might be otherwise undetected by optical sensors. As seen in 1, SAR imagery clearly highlights water features that optical sensors struggle to pick up. SAR is also an all-sky sensor, meaning that it operates regardless of light conditions, and its wavelength range is large enough that it penetrates cloud cover, which helps provide continuous spatial coverage in geographic areas that might otherwise be occluded to optical satellite sensors due to cloud cover [7], or polar regions that lack sunlight for half of a year.

SAR is predated by passive microwave sensing, which monitors similar microwave frequencies in order to pierce cloud cover but does not emit a signal of its own in order to do so. As a result, passive microwave sensing offers much lower resolution compared to SAR. Sensors such as AMSR [86], AMSR-2 [1], SMAP [26], and GPM [66] all passively monitor microwave signals emitted from the Earth. By comparison, SAR actively beams energy down to Earth's surface and records the response, which allows for multiple polarizations at transmission and reception. Polarization describes the orientation of the plane that the electromagnetic wave oscillates on. The shorthand for polarization is the orientation of the emission, which is either vertical (V) or horizontal (H), followed by the orientation of the reception, which will also be either vertical or horizontal. Each polarization results in the waves scattering differently upon reflection, enabling certain polarizations to be particularly effective at picking up certain types of surface features. For example, the VV polarization is good at picking up rough surface scattering, typically caused by roughened water or vertical surfaces. HV or VH polarizations are good at picking up volume scattering, where the signal bounces around a number of times in a given volume before being broadcast back out to space; this is typically caused by forest canopies and vegetation. We see in figure 1a and figure 1b the the VH polarization provides more fine-grained details in a variety

of forested areas than the VV polarization, where those areas are whited out. HH polarization is good at picking up horizontal surfaces, such as smooth ice or calm water.

Compared to optical imagery, SAR captures distinct and complementary information, despite it also being stored as a raster (gridded) data type. The different frequencies of SAR, the different polarizations, and the volume scattering aspect make it stand apart from optical. For instance, surface reflectance of sea ice will appear as a bright surface in optical imagery, regardless of its age (which is a proxy for its thickness and level of hazard it poses to marine navigation). However, as sea ice ages (from thinner first-year ice to thicker multi-year ice), its salinity changes, and because of SAR's volume scattering (caused by salt content and air bubbles in ice), the appearance of thick ice changes in SAR imagery compared to younger, thinner ice [70]. This is the primary reason sea ice analysts primarily rely on SAR imagery in making sea ice charts, and use optical only as a secondary reference. As we demonstrate later in this manuscript, this complementary aspect of SAR imagery (despite it being stored as an image) motivates incorporating this multi-sensor information into RS foundation models.

2.3 Non-Image Data

Due to the ubiquity of the raster image format in remotely sensed data, current RS foundation models tend to be focused on using images to train, but a variety of other modalities do exist. Text, geographic location, and digital elevation maps (DEM) are all among potential additional modalities available in remote sensing at scale, and it is conceivable that derivative information products such as population movement trajectories, social media data, and vector maps may be incorporated in enhancing foundation models. Any dataset with sufficient spatial coverage that contains geographic coordinates and a timestamp can feasibly be compared with corresponding satellite imagery in order to further improve a model's ability to interpret how satellite imagery pertains to ground level information, resulting in a broad swathe of different modalities available for RS models to leverage. With an eye on these additional potential modalities, the rest of this manuscript focuses on the present and immediate future of foundation models in remote sensing with fundamental design and recommendations to advance the field.

3 Foundation Models Originating in Computer Vision

This section presents a broad overview of the techniques used by current foundation models in CV, many of which serve as the bedrock for RS foundation models today [60].

3.1 Negative Sampling Models

One successful approach to SSL in CV is contrastive learning via negative sampling [14]. Contrastive learning augments one image in two different ways, then a model is trained to recognize whether two images are augmentations of each other, i.e., are a positive pair. Any images that are not augmentations of one another are defined as negative pairs. For every batch, an image will have only one positive pair, and $n-1$ negative pairs, where n is the batch size. This approach can be thought of as a classification task where the model trains on classifying two augmentations as either a positive or negative pair. Within a given batch of samples, normalized-temperature cross entropy loss (NT-Xent loss) [14] pulls together embeddings from the same origin and pushes apart embeddings that came from different origins, resulting in an encoder that learns sophisticated embeddings of images without the need for supervised learning. The encoders then can be ported to other downstream tasks, while reducing the need for labeled samples.

SimCLR [14] achieved great success with this approach; SimCLR trained on ImageNet ILSVRC-2012 [78] and introduced a non-linear projection head to improve the embedding quality of the layer before it. They also discovered

that augmentations like color jitter and random cropping were particularly effective in forcing the model to learn embeddings that represented the data as a whole, not just dominant features like color distribution. Momentum Contrast (MoCo) [34] also utilizes contrastive learning, but maintains a dynamic memory bank or queue of negative samples, and updates it using a momentum encoder. This approach allows MoCo to effectively utilize smaller batch sizes than SimCLR, reducing memory requirements. Contrastive Language Image Pre-training (CLIP) [73] is a contrastive learning framework that treats the text modality as a naturally occurring augmentation of a given image and trains two encoders, one for the text modality and one for the image modality. Given the multi-modal nature of this approach, contrastive learning to bring positive pairs together results in an alignment of the two modalities in the same embedding space. All of these models introduce concepts that have been leveraged by recent foundation models within the RS domain [95].

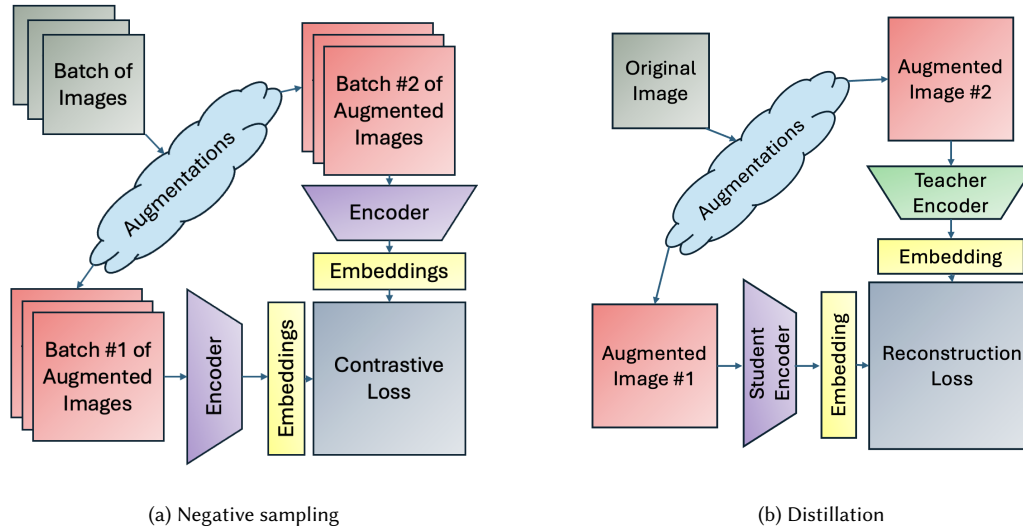


Fig. 2. CV foundation model architectures that leverage contrastive learning.

3.2 Distillation Networks

While contrastive learning via negative sampling achieves SOTA performance in CV, it generally requires large batch sizes in order for the loss to effectively contrast against a large number of negative samples. The need for a large batch size results in significant hardware requirements, which is an obstacle to research for many teams. Distillation networks such as Bootstrap Your Own Latent (BYOL) [31] and Self-Distillation with No Labels (DINO) [9] were developed to address those hardware constraints.

Whereas negative sampling approaches can be thought of as a training on a classification task, distillation networks use a generative task as their objective. Distillation networks contain two encoders, dubbed the “teacher” and the “student”. Both are fed in augmented versions of an image. The teacher encoder outputs an embedding, and the student encoder is paired with a decoder that is responsible for generating a matching embedding. Then, generative loss is performed between the teacher and student embeddings and back propagated into the student network. The teacher network learns via the weighted average update system that was introduced in MoCo.

The generative nature of the student network’s task forces the student network to learn effective representations without requiring negative samples. This method reduces the reliance on large batch sizes and extensive memory, making it more resource-friendly. It also outperforms comparable negative sampling models with fewer parameters [31]. However, there is possibility of embedding collapse, as both the teacher and student networks learn based on the same loss [15]. Embedding collapse describes a condition where a model generates embeddings that span a low-dimension subspace of the latent space, sometimes becoming so extreme as to only span a single point; this represents a significant loss of ability to capture information in embeddings [46]. The asymmetry introduced by the weighted average update system for the teacher network prevents embedding collapse, but this phenomena is not well understood.

3.3 Masked Auto-Encoders

The Masked Auto-Encoder (MAE) approach is prevalent in NLP foundation models, such as BERT [49] and GPT [69]. The notion is that by masking parts of a sample, running the masked sample through an encoder, then asking a decoder to reconstruct the original sample from the resulting embeddings, the encoder learns effective embeddings of the data. This approach has recently been extended to CV with models like MAE [33] achieving SOTA performance. As with contrastive learning approaches, MAE takes steps to ensure that learned embeddings are representative of the data as a whole. This takes the form of masking roughly 75% of the data to prevent trivial reconstruction from patch context [33]. The generative nature of the task, like that of distillation networks, means that the batch size can be relatively small, making it relatively resource-friendly with moderate computing resources.

Masking approaches with established frameworks, such as Convolutional Neural Networks (CNNs) or Recursive Neural Networks (RNNs), replace a patch with a mask token, then feed in the whole image, including masked patches, into a network. But the usage of ViTs, which include positional embeddings as well as patch embeddings, allows for training pipelines to only feed encoders unmasked patches, shrinking the size of the necessary input layers and dramatically speeding up training time [33]. Similarly, utilization of a lightweight decoder also forces the encoder to learn more accurate representations while speeding up runtime [33]. These optimizations mean that the MAE approach scales remarkably well, resulting in models that can contain billions of parameters [25]. Current CV research has identified a gap in the number of parameters between SOTA NLP and CV models and plans to improve the parameter count in CV foundation models even further [25].

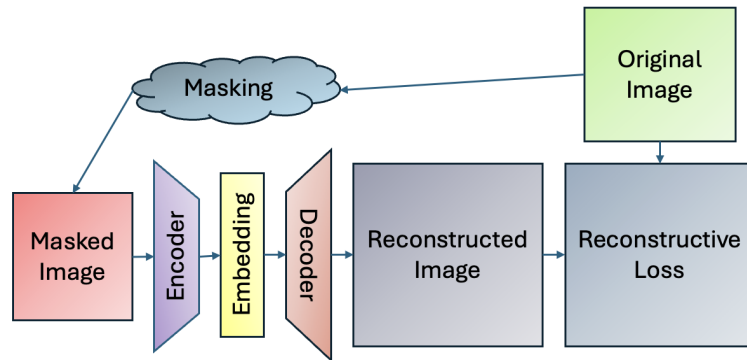


Fig. 3. CV foundation model framework for masked auto-encoding

4 Negative Sampling Models in Remote Sensing

While the underlying principles of negative sampling generally remain the same from augmentations applied in CV to RS, the shared location of different imagery acquired at different times or by different sensors enables RS models to lean heavily on different sensors' imagery or same sensor's different temporal passes as naturally occurring augmentations of the same image [41]. This enables two main advantages: it lets a model leverage and fuse imagery that comes from different RS sensors or different temporal acquisitions that is available for the same locations, and it reduces the time required to do hyper-parameter tuning for augmentations. The latter often adds significant overhead to training contrastive learning approaches [42].

4.1 Temporal Acquisitions as Augmentation

Pre-trained on RGB bands from Sentinel-2, Seasonal Contrast (SeCo) [64] borrows heavily from SimCLR's general framework and outperforms CV models such as MoCo on downstream land cover classification tasks, indicating that there is implicit benefit in creating foundation models for the remote sensing domain as opposed to borrowing models directly from the computer vision field. Instead of creating hand-crafted image augmentations outlined in SimCLR [14], such as color jitter or gaussian blur, SeCo treats images of the same location at different points in time as natural augmentations of one another. However, SeCo does not simply rely on natural augmentations; it also utilizes random cropping, random flipping, and color jitter to prevent the model from learning trivial representations of the data. The resulting model is essentially season- or time-agnostic, meaning it provides a general representation of data regardless of acquisition-time-of-year. While this is helpful in identifying land cover or land use which does not change from season to season, it may not fit scenarios where retaining seasonal differences in embeddings for downstream tasks is essential, such as time series forecasting for projecting forest fire recovery in an area.

SeCo's approach of contrastive learning between spatially aligned, temporally different RS image pairs has also been explored in Geographically Aware Self Supervised Learning (GASSL) [3]. However, this approach trains on the Functional Map of the World (FMoW) [19] dataset, which contains multispectral imagery from the DigitalGlobe constellation [2], and does not utilize any additional artificial augmentations. In addition to the contrastive task, GASSL also leverages the metadata available in RS imagery for a SSL task. This approach clusters together images by location and then predicts the latitude and longitude present in the metadata; the combination of this task coupled with contrastive learning across geographically aligned images results in a framework that attempts to explicitly learn time-agnostic representations of a given place. As with SeCo, the authors note that this approach learns temporally invariant features, but may struggle with tasks such as change detection [3]. Unlike the approaches below, latitude and longitude are not pre-processed in any way or treated as an additional modality.

4.2 Geographic Location as Augmentation

Explicitly utilizing spatial data such as latitude and longitude provides value, but purely introducing them as features can result in models that perform poorly when asked to generalize to locations not within their training data [44, 48]. Therefore, a new generation of models dubbed "location encoders" have emerged, which once trained, take in latitude and longitude, then return an embedding of that location that quantifies and summarizes ground conditions of that location. Several models in this generation of location encoders rely on the CLIP framework [73] and treat 'location' as one modality, with a location-specific encoder to use in contrastive learning. This location encoder, in turn, distills the information extracted from the other mode, often an image obtained at that location.

GeoCLIP [11] uses images taken at ground level from Flickr for one modality and spatial encodings for the other modality, then uses CLIP’s contrastive learning objective to learn effective representations of each modality. GeoCLIP uses Random Fourier Features (RFF), which have been shown to be highly effective in memorization and image reconstruction [87], in order to store features learned from images into the location encoder. These Random Fourier Features allow GeoCLIP to learn high quality spatial encodings that capture information from the ground level photos.

Contrastive Spatial Pretraining (CSP) [63] also performs contrastive learning between ground level imagery and locations, but it explores a variety of techniques for generating positive and negative pairs that are explicitly tailored to spatially distributed data. In addition to CLIP’s standard in-batch negative sampling, CSP utilizes random negative location sampling, in which negative pairs for an image are generated by uniformly sampling locations at pre-training time; in this instance, the positive pair is still the corresponding location for the image. CSP also explores SimCSE-based sampling [30], in which two location encoders are initialized the same, but utilize different dropout masks. In this case, the same location is fed through each location encoder, and embeddings that point to the same initial location are considered positive pairs, while all other combinations are considered to be negative pairs. Each sampling approach forms a component of CSP’s contrastive loss function, resulting in a framework that learns nuanced representations of each modality.

SatCLIP [48] also follows the CLIP approach while utilizing spatial encodings as one of its modalities and optical imagery captured from Sentinel-2 as the other. SatCLIP takes in all Sentinel-2 bands and does not limit itself purely to RGB data. SatCLIP does not utilize Random Fourier Features for the spatial encodings, and instead uses a SirenNet [81] that relies on spherical harmonics [79] to learn effective spatial encodings.

Geo-Aligned Implicit Representations (GAIR) [56] takes this a step further by utilizing location as a way to align multispectral satellite images from Sentinel-2 and ground-level RGB images from the Global StreetScapes dataset [38]. Ground-level imagery can provide a highly informative mode to train satellite imagery against, but a single satellite image’s scope is so large that hundreds or thousands of ground-level images can correspond to a single satellite image. In order to address this issue from a contrastive learning standpoint, GAIR learns Implicit Neural Representations (INR) [101] of a Sentinel-2 image. INR learns a continuous function for spatial coordinates to corresponding signals. These INR encodings of Sentinel-2 imagery are then contrasted against location encodings and ground level vision encodings. GAIR uses RFF [87] for location encodings and a standard ViT for ground-level image encodings.

4.3 Different Sensors as Augmentation

Multi-modal SimCLR [42] treats images of the same location from different sensors as naturally occurring augmentations. This approach has two encoders: one trained on RGB bands of Sentinel-2, and one trained on VV and VH polarizations of SAR images from Sentinel-1. As with SeCo, this approach does not rely entirely on natural augmentations. It adds random cropping, flipping, color jitter/drop, and gaussian blur, all augmentations that have proven useful in other remote sensing models [41]. Interestingly, fine-tuning Multi-modal SimCLR on downstream tasks with a dataset of only one modality, either Sentinel-1 or Sentinel-2, yields better results compared to other methods that train only on the one sensor [42]. This indicates that leveraging the additional modalities (i.e., sensors) present in remote sensing for SSL has the potential to result in better representations of a single modality in the modality-specific encoder.

Contrastive Radar-Optical Masked Auto-encoders (CROMA) [28] also performs SSL on Sentinel-1 and Sentinel-2 data, training an encoder for each sensor. However, CROMA takes inspiration from the FLIP framework [45], which independently masks each mode of data before feeding them into encoders and performing contrastive learning in the standard CLIP [73] setup. Masking images before encoding them results in a significantly less memory intensive process

than encoding the raw image when vision transformers are used. Therefore, the FLIP framework enables contrastive training with a much larger batch size with the same or less memory footprint, which results in faster convergence. CROMA implements this approach with remotely sensed images, contrastively learning between masked Sentinel-1 and Sentinel-2 images. CROMA also introduces a third encoder that takes in concatenated Sentinel-1 and Sentinel-2 encodings, generates multi-sensor encodings, then is fed into a multi-sensor decoder responsible for constructing the initial Sentinel-1 and Sentinel-2 images. In this manner, CROMA is able to introduce contrastive and reconstruction loss terms into their framework, resulting in a model that effectively learns uni-sensor representations for Sentinel-1 and Sentinel-2 and multi-sensor representations of both Sentinel-1 and Sentinel-2. This framework is benchmarked against BigEarthNet [84] and FMoW [19] classification tasks, demonstrating SOTA performance with images from a single sensor and multi-sensed images. BigEarthNet contains roughly half a million Sentinel-2 images where each patch can have multiple land-cover classes. CROMA also utilizes modified ALiBi positional embeddings [72] for their ViT encoders; these embeddings provide an advantage over standard sinusoidal positional embeddings by biasing the embeddings based on Euclidean distance between key-query pairs, thus imbuing the embeddings with a degree of spatial awareness.

4.4 Text as Augmentation

CLIP’s original design used text and images as its two modalities, and RemoteCLIP [55] goes back to these roots. RemoteCLIP takes in text as its one modality, leaning on image captions to generate natural labels. Other models’ requirements for additional fine-tuning, as opposed to zero-shot utilization, motivates this model’s development, as including text as one of the modalities results in good zero-shot performance downstream [107]. This model treats RGB images taken from Sentinel-2, drones, and other aerial platforms as one modality. This variety in the sources for the image modality is designed to result in a more robust encoder that will be resolution agnostic, yet the reported performance takes note of RemoteCLIP’s struggles with zero-shot image classification as an indication that there is additional work to be done in that regard.

For the text modality, RemoteCLIP relies on image captions already present in the human-annotated satellite imagery datasets. Where no captions are paired with an image, a preprocessing stage generates appropriate text annotations. This preprocessing stage performs standard object detection on the image, then uses a script to programmatically generate a corresponding sentence, which is then used as the positive text annotation. Generating captions via script will lack natural variance that is present in a typical corpus, and generating these captions via NLP processes such as ChatGPT will inherently introduce extrinsic noise and potential bias into the dataset. Nevertheless, RemoteCLIP outperforms SOTA models like CLIP and DINOv2 in zero-shot evaluation of object counting in the Remote-Count dataset [29], and few-shot classification of 12 RS benchmarks, including EuroSat [36], RSC11 [104], and RESISC45 [18], which indicates that descriptive text as a modality has definite value in the remote sensing domain.

Given multi-modal foundation models’ origins as VLMs, there are a variety of other RS foundation models that leverage text as a modality in order to enable few-shot learning capabilities. These models have been surveyed by [105].

5 Distillation Networks in Multi-Modal Remote Sensing

One successful example of a distillation network in the RS field is RS-BYOL [42], which borrows BYOL’s framework and uses the multi-modal aspect for multi-sensor remote sensing data. Just as with negative sampling approaches in RS, different sensors’ imaging of the same location are leveraged as natural augmentations of the same image. One modality is drawn from Sentinel-2 optical, whereas the other is drawn from Sentinel-1 SAR. Similarly, additional

augmentations of random crops, rotations, color jitter, and grayscale are applied to prevent the model from learning trivial representations of the data.

RS-BYOL utilizes 10 bands of data in Sentinel-2 with 10-20 m resolution and the VV and VH polarizations of SAR present in Sentinel-1. The model outperforms negative sampling approaches such as SeCo in linear probing when all bands are present from Sentinel-2, indicating that there is inherent value in incorporating multispectral bands from Sentinel-2 in addition to the RGB bands. However, SeCo outperforms RS-BYOL with linear probing when only the RGB bands are present, indicating that negative sampling approaches may still have a performance edge in remote sensing. The lighter resource requirements for distillation networks reflects a tradeoff between model performance and hardware requirements.

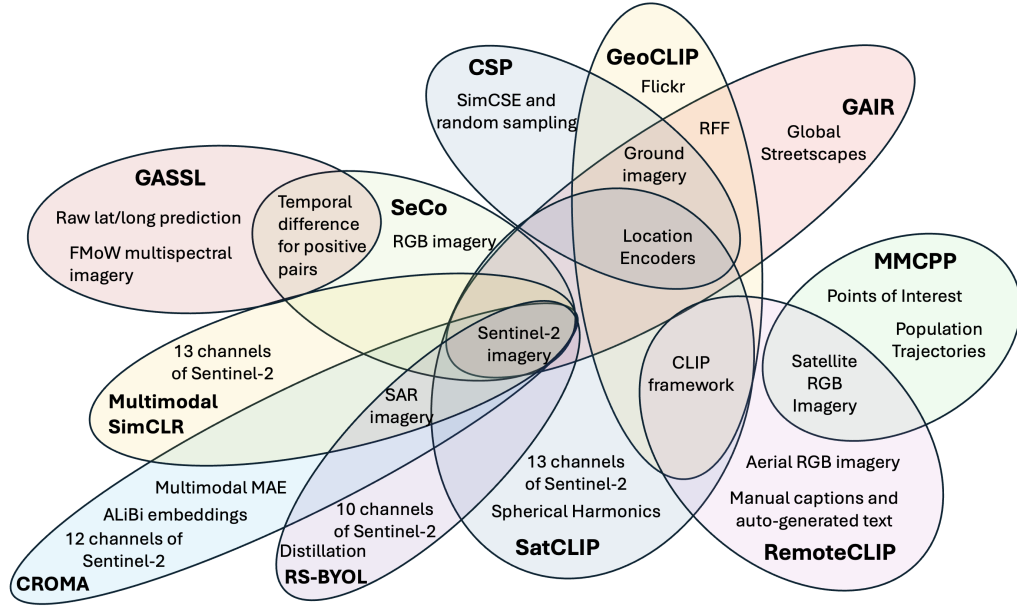


Fig. 4. An illustration of shared and unique concepts among RS foundation models which utilize contrastive learning for their SSL task.

6 Masked Auto-Encoders in Remote Sensing

While MAE is a powerful approach in CV, it requires significant adaptations to be effectively leveraged in the RS world. Below are some of the adjustments that have been made to MAE in order to leverage it more effectively in the remote sensing domain [67].

6.1 Masking Approach

The simple CV approach of masking individual patches of an image fails to work effectively with RS imagery [85]. Compared to natural images in CV, satellite and aerial images in RS often capture small surface features, dense objects, complex backgrounds, and a range of possible object orientations. Similarly, natural images tend to follow expected proportions with well-defined distributions, whereas the same cannot be said for RS images [75]. Sun's Remote Sensing

Foundation Model (RingMo) introduces PIMask [85] to account for these inherent differences, as masking an entire patch of a RS image might lose information that is unique to that given patch. Therefore, some pixels in each masked patch are randomly preserved, and multilayer convolution is applied to each patch. Compared to traditional CV methods, where masking 50% of an image would completely mask 50% of the patches, masking 50% of an image with PIMask would partially mask a higher percentage of patches. The overall number of pixels masked in the image would still be 50%, but the spatial distribution is different.

MAE in CV finds that masking high percentages of the image (roughly 75%) results in more accurate representations being learned [33], and that carries over to the current implementations of MAE in remote sensing as well [85]. This parallels with the findings from negative sampling approaches that making the pretext task with contrastive objective more difficult via multiple augmentations results in the model learning better embeddings. RingMo’s embeddings outperform embeddings generated with comparable MAE frameworks and standard CV patch masking, underscoring the importance of improving the masking procedure for satellite imagery.

Spatial-Spectral MAE (S2MAE) [53] takes this a step further, as they find that masking 90% of satellite imagery yields the best results in their novel framework. S2MAE trains on multispectral imagery from FMoW [19] and BigEarthNet [84] datasets. Unlike RingMo and other image RGB masking strategies which mask out the same pixel across all channels, S2MAE employs independent 3D masking, which masks out different pixels in each channel. 3D masking was introduced for videos and appears to learn environmental details well, but struggles to track movement from frame to frame [27]. While this is poorly suited for video analysis, it is ideal for RS applications, as seen in S2MAE’s SOTA performance on the Onera Satellite Change Detection (OSCD) [24] dataset and EuroSat [36]. S2MAE also finds that shallow decoders are poorly suited for SSL with multispectral imagery, a notable departure from established CV practices [33].

6.2 Temporal Encodings

SatMAE [22] leans on MAE’s utilization of a ViT as the backbone, but encodes the hour, month, and year as temporal encodings, then concatenates these transformed temporal encodings to the standard positional encodings that are innate to the functioning of a ViT. As with SeCo, the inclusion of temporal information in self-supervised learning for RS foundation models can have substantial performance improvements, but it also means that the embeddings learned are agnostic to temporal variability, i.e., learning an average of variations over time, thus limiting the value for certain downstream tasks where preservation of temporal nuance is crucial. Still, this ability to encapsulate temporal data highlights the flexibility of the MAE approach in remote sensing.

Taking into account the adjusted positional encoding, SatMAE experiments with different masking approaches. It utilizes consistent masking, where the masked regions are spatially-consistent across all images of a given location, and independent masking, where the location of the patches can change from image to image of a given location. Results indicate that independent masking can trivialize the task, as the model might be able to reconstruct a given masked patch by referring to an unobstructed view of that patch at a given time, so a random cropping augmentation is applied to ensure the model learns robust embeddings.

Prithvi [43] trains on the Harmonized Landsat Sentinel-2 (HLS) [21] dataset, which contains multispectral images captured by Landsat 8/9 and Sentinel-2 in order to provide a satellite imagery dataset with higher temporal resolution. Prithvi leverages this higher temporal resolution to arrange these 2D images in a time series and updates the traditional MAE positional and patch embeddings to be 3-dimensional, where the third dimension pertains to time. When masking patches, they specifically apply 3D convolutions to avoid losing information specific to any one given patch, similar

to RingMo’s [85] approach. Aside from the incorporation of temporal data, Prithvi also utilizes a landscape stratified sampling strategy to avoid bias towards more common ecosystems or landscapes.

Presto [90] takes this approach even further, constructing a pixel-timeseries training dataset that consists of input from multiple types of data, including Sentinel-2 RGB, Sentinel-1 SAR, DEM, and the Dynamic World [6] dataset, which contains land cover labels for 10m resolution Sentinel-2 imagery. The framework then employs a variety of different strategies for training, masking channels, blocks of timesteps, single timesteps, and/or random pixels for reconstruction by a downstream encoder. The resulting encoder is performant with regards to feature extraction, fine-tuning, and time series forecasting. The variety of masking strategies employed ensures that Presto can successfully process time series datasets with missing channels, a variety of temporal resolutions, and only a small subset of timesteps. However, performance on tasks that are temporally agnostic and rely on a single image lags behind SOTA models; the authors note that this is possibly due to the model’s inability to process images with a spatial resolution higher than 10m.

6.3 Scale

Foundation models in CV, and most foundation models in RS by extension, process images in local image coordinates, meaning that the learned representations are dependent on the scale and resolution of the satellite sensor. ScaleMAE [74] is designed to address this issue by scaling the image coordinate system such that it matches the actual spatial scale of objects, ensuring that patch size, as measured in geospatial units, is the same across various images. This is done via introducing a Ground Sample Distance (GSD) positional encoding, which then informs the ViT of both the geospatial scale and image position of the patch. Put differently, ScaleMAE addresses relative spatial scale, but does not incorporate absolute geolocation in its training. As with SatMAE, ViT’s framework, with dual patch and positional encodings, lends itself well to introducing the concept of scale to the model.

Dovetailing with the incorporation of scale, ScaleMAE’s decoder produces both high and low resolution images in order to capture both low-frequency features, such as mountains and rivers, and more fine-grained high-frequency features, such as vegetation. It does so by utilizing a Laplacian-pyramid decoder instead of the standard transformer decoder.

6.4 Multiple Decoders

MAE is originally designed to take in a single modality, which can make it challenging to utilize the different sensors that are available in remote sensing. By comparison, contrastive learning models elegantly use different modes of data available by creating an encoder per modality. MMEarth [67] explores a potential multi-modal MAE approach by pairing an encoder for one modality with many modality or task-specific decoders. MMEarth takes in multispectral data from Sentinel-2 that contains all 13 bands, masks that data, then utilizes an encoder to generate embeddings. Typical MAE would pair this with a single decoder designed to reconstruct the original optical image. Instead, MMEarth pairs the optical encoder with 12 separate decoders. Six of these decoders are focused on pixel level tasks, such as reconstructing a corresponding optical image, a corresponding SAR image, or a corresponding Dynamic Earth image. The other six decoders are focused on image level tasks, such as classifying the corresponding biome or month.

The loss for all of these decoders is back propagated into the encoder, resulting in representations of optical imagery that capture data from other modes. While this approach learns refined optical representations and therefore, a good encoder for optical imagery, contrastive learning approaches of a similar manner would also learn encoders for the other modes of data. Depending on the downstream tasks that are required, this may be a significant limitation for MMEarth’s effectiveness.

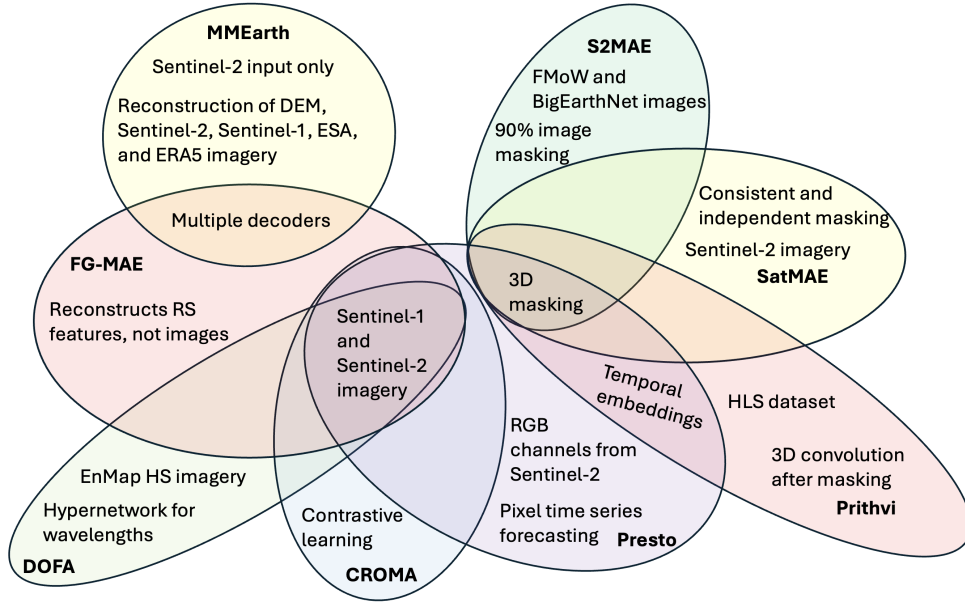


Fig. 5. An illustration of shared and unique concepts among RS foundation models which utilize masked auto-encoding for their SSL task and train on multispectral and/or multi-sensor data.

Feature Guided MAE (FG-MAE) [96] also explores the utilization of multiple decoders for MAE, but does so by tasking the model to reconstruct specific features of interest in the remote sensing world. MAE’s focus on pixel-level details can limit the model’s capability in understanding satellite imagery. FG-MAE explores a variety of reconstruction objectives, including Histograms of Oriented Gradients (HOG) [23], Normalized Difference Indices (NDI) such as Normalized Difference Vegetation Index (NDVI) [39], CannyEdge [8], and Scale-Invariant Feature Transform (SIFT) [58]. FG-MAE maintains two separate models: one for optical imagery and one for SAR imagery. In EuroSat [36] and BigEarthNet [84] classification tasks, FG-MAE’s optical model demonstrates comparable or better results to standard MAE when only reconstructing a single one of these RS features. However, performing reconstruction on both HOG and NDI results in a substantial performance boost compared to standard MAE. FG-MAE’s SAR model finds that simply reconstructing HOG yields the best results, as it tends to work well with the noisier Sentinel-1 imagery.

6.5 Orientation Awareness

In natural imagery, the orientation of objects is of importance; if an object is upside-down, that is semantically different compared to the same object right side up. By comparison, the same object can appear in satellite imagery in a variety of different orientations, and those orientations have little to no semantic differences. Leveraging the standard MAE approach from CV treats these orientations differently, which is not desirable for remotely sensed images.

Masked Angle-Aware Auto-Encoding (M3AE) [54] emerges to address this particular problem. M3AE trains on the MillionAID dataset [57], an RGB dataset derived from Google Earth imagery, and introduces a scaling center crop augmentation to every image, resulting in an augmented image where an object in the center will be rotated into a different orientation from the original. This augmented image is masked then fed into an encoder-decoder framework

where the decoder attempts to reconstruct the original image. In order to ensure that the model pays attention to the re-oriented object, the encoder is fed positional embeddings that include a third dimension which tracks the angle of a given patch. M3AE also introduces an optimal transport reconstruction loss to automatically assign similar image patches for each rotated crop patch; this ensures that the rotation is taken into effect from a loss standpoint.

Rotated Varied-Size Attention (RVSA) [93] also develops a novel approach to developing orientation-agnostic representations of RS imagery, but does so through ViT self-attention compared to image augmentation. Trained on the MillionAID dataset [57], RVSA shifts away from the standard multi-head self-attention (MHSA) present in traditional CV ViTs, as full attention scales quadratically to image size. Given the potential high-resolution nature of RS imagery, RVSA leverages a varied-size window-based MHSA (VSA), where images are partitioned into non-overlapping windows, then have MHSA applied [102]. In order to learn orientation, RVSA randomly rotates and re-sizes these windows before performing self-attention within a ViT. With these self-attention tweaks in effect, standard MAE is employed for reconstruction masked MillionAID images. The result is a framework capable of swiftly handling high resolution RS imagery that learns orientation-agnostic representations of RS imagery.

While orientation matters a great deal for object recognition in RS imagery, the M3AE authors notes that this applies predominantly to man-made objects [54]. These representations are likely better suited for urban or developed environments, and development of a training dataset specifically focusing on man-made objects would likely be useful for model fine-tuning.

6.6 Wavelength Awareness

The variety of different satellite sensors available means that even if two sensors monitor the same rough wavelengths, their spectral resolution or means of acquisition might be very different. For example, Landsat-7 and Sentinel-2 are both considered multispectral and monitor visible to SWIR wavelengths, but Landsat-7 splits that into 8 distinct bands, compared to Sentinel-2's 13 bands. As a result, a foundation model trained on Sentinel-2 data would not be well-suited to work with Landsat-7 data out-of-the-box, and vice-versa.

Dynamic One-For-All (DOFA) [100] attempts to address this problem by creating a framework that can take in data from any number of different sensors. DOFA follows a hyper-network approach [13], where a hypernetwork takes in the wavelength details of a given band and then generates weights that are used to initialize a downstream neural network. A monochrome image of a single band is masked, then fed into that neural network to generate an encoding. That encoding is then fed through an encoder-decoder structure responsible for reconstructing the original monochrome image of that band. This framework is designed to learn bandwidth specific features via the hyper-network and shared features via the shared encoder-decoder. DOFA is trained on SAR imagery from Sentinel-1, multispectral imagery from Sentinel-2, hyperspectral imagery from enMAP, and high resolution RGB imagery from NAIP. The resulting framework achieves SOTA performance on downstream tasks such as BigEarthNet [84], So2Sat [106], and EuroSat [36].

While this framework is highly promising in its potential applications to downstream tasks on imagery acquired via a sensor not in the training set, this ability is unfortunately still largely theoretical, as it is not thoroughly explored in the published results [100].

7 Future Considerations

Given the relative youth of foundation model development in RS, there is a high degree of fluidity in existing frameworks and overall goals.

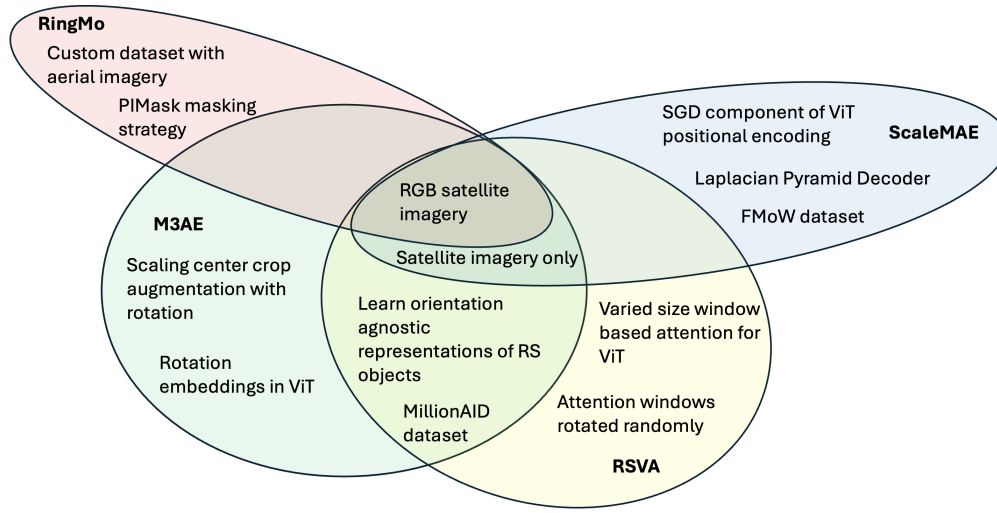


Fig. 6. An illustration of shared and unique concepts among RS foundation models which utilize masked auto-encoding for their SSL task and all train only on RGB images.

7.1 Learning Representations in the Era of Climate Change

Given the rapidly shifting nature of the Earth’s climate, learned representations should be robust enough to take these changes into account without substantial retraining. Otherwise, the re-usability of these representations becomes less desirable or reliable over time, diminishing one of the main benefits of the encoder-decoder approach. When considering the variety of modalities present in RS, there is the potential to create representations that can withstand the challenges of a changing climate, but a degree of care is required. Relying too heavily on geographic locations and temporal data could very well result in representations that quickly become outdated as the world’s climate shifts. For example, a learned representation of a specific location on a coastline could cease to be relevant due to rising sea levels. Similarly, climate change has resulted in marked seasonal shifts within the past decade, so learning representations of what a given location looks like at a given time of year may wane in relevance as well.

Careful consideration is needed to either weigh temporal and geographic data in the appropriate manner or create a framework that allows for lightweight retraining of modalities that are dependent on a particular time and space, given that climate change perpetually recontextualizes a given scene in time and space. By comparison, representations based on modalities that directly observe the Earth, such as satellite imagery and text, should be more tolerant to climate change-induced drift, as their representations are tied to understanding underlying observations directly within the data itself and are less reliant on climate context. Given that many remotely sensed datasets date back decades, there is merit in creating foundation models that perform time-series forecasting over long time periods in order to effectively learn representations which take long-term trends into account. This historical data also opens the door for assessing the capability of remote sensing foundation models to quantify historically understood climate and biome changes.

7.2 Under-Tapped Modes for Geospatial Representation Learning

Much of the current research focuses on drawing parallels to the work done on CV foundation models. Given the success of foundation models in the CV domain and the sheer amount of imagery that is available, be it from satellites or other aerial sources, this is a necessary first step. However, models such as MMCP [17] use the CLIP contrastive learning objective and rely on other modalities, such as trajectory maps, points of interest, and aerial images. Their success should serve as a somewhat cautionary tale against becoming too invested in foundation models that purely focus on satellite and/or aerial imagery. Environmental stations measure features such as groundwater, weather, or snow melt data, and provide important climate and atmospheric information at a very high temporal resolution, often recording data on a daily or even hourly basis. More human-centric data, such as social media posts, social connectedness indices [4], and trajectory data, also provide invaluable information for understanding more societally-focused downstream tasks. Both forms of information are not observable from space, but could provide useful modes due to their different perspective and high temporal resolution. Data on rapidly changing phenomena also tends to not be observable from space, as changes can occur too quickly for a satellite to capture, due to orbit and revisit time. GAIR [56]’s usage of INR representations for satellite imagery also provides a useful starting point for ensuring that granular, ground-level data can be effectively mapped to learned representations for satellite imagery.

7.3 Performance versus Training Expenses

Given the computational costs of training transformer models, the training expense of foundation models has rapidly become an obstacle across a variety of domains, with some models now including a section on carbon footprint [22]. Given that a substantial portion of downstream tasks for remote sensing pertain to combating the negative effects of climate change, there is a compelling argument for remote sensing foundation models to focus on curtailing training expenses. Massive models which create a large carbon footprint ultimately may be counterproductive from a climate change standpoint. However, the perpetual flow of remotely sensed data which dates back decades also encourages exploring the development of an incremental learning pipeline to efficiently fine-tune foundation models with up-to-date information.

Aside from a carbon footprint perspective, models with huge numbers of parameters have their downstream applications somewhat limited due to computational requirements. Some models, such as MOSAIKS [76], focus on lightweight frameworks in order to promote access to remote sensing foundation models. MOSAIKS has competitive results on a number of downstream tasks, indicating that increasing parameters within models may follow a law of diminishing returns. On the other hand, the encoder-decoder structure that is predominant in foundation models allows for repeated, diverse usage of representations on downstream tasks. Arguably, leveraging significant resources to generate high quality embeddings as a one-time cost is the most effective path moving forward, as this approach results in SOTA performance on downstream tasks with relatively few resources necessary for future fine-tuning.

It is possible that distillation networks may provide a happy medium between the desire for high quality embeddings and lower computational requirements. While models such as RS-BYOL [41] have demonstrated that such an approach is feasible with remotely sensed imagery, distillation has yet to be explored as a SSL approach in remote sensing to the degree that masked auto-encoding or contrastive learning with negative samples have been. The recent and well-publicized success of DeepSeek [98] in the NLP field highlights the viability of distillation as a SSL approach and indicates that it should be further examined within the remote sensing domain.

7.4 Directions for Framework Development

Many of the foundation models covered in this manuscript leverage a variety of different objectives that force the encoder to learn accurate representations of the data and test on downstream generalizability. Most of these models use a single pretext task training objective in the hopes of generating a general representation. In other domains, such as NLP, multiple pretext tasks are optimized simultaneously as a key part of learning generalizable embeddings [49]. RS foundation models could profit from a similar strategy.

MMEarth [67] utilizes multi-task training, as the model uses a variety of downstream decoders for different modalities that each backpropagate loss to the same encoder. FG-MAE [96] takes this a step further by tasking decoders to not just reconstruct a different modality, but to reconstruct specific RS feature maps pertaining to the masked training image. Future research can investigate models that marry these MAE approaches with contrastive learning. Training a MAE encoder per modality, then performing contrastive loss between the resulting encoders could provide a powerful boost in representation learning, as both objectives learn invariant features in very different ways. Current foundation models that take text in as a modality inherently use this approach somewhat, as they rely on pre-trained NLP transformers, which have performed Masked Language Modeling training already for their text encoders [49]. CROMA [28] begins to explore this possibility in the RS domain by contrasting two independently masked images, but this is explored mainly for performance reasons, and the MAE objective is on multi-sensed image embeddings as opposed to MAE for each sensor. This approach may scale poorly with the addition of more sensors due to input size. Similarly, the nature of a MAE task shared with multiple modalities seems to align these sensors more closely, rendering it somewhat redundant to the contrastive task already being executed.

Most multi-modal models in the RS domain only consider two to three sensors, but the sheer number of modes available means that it would be beneficial to have a model that is capable of scaling effectively to learn representations that capture a dynamic number of modes. MMEarth’s innovation of having a decoder per mode is promising in that regard, but it runs into the problem of only learning embeddings for one sensor. While contrastive learning can theoretically be applied across a variety of modes, the cost of training a separate encoder per sensor could quickly result in resource challenges. Ultimately, a multi-modal framework that is capable of learning representations for multiple sensors without explicitly requiring that every mode has its own encoder would be ideal, but careful consideration is required to develop a framework that is both flexible and robust enough. DOFA’s [100] hypernetwork-inspired framework is promising in that regard due to its ability to handle a variety of different sensor inputs in pre-training, but it fails to take into account whether a wavelength is being actively sensed or passively sensed, which affects the nature of the imagery. Similarly, the various polarization of SAR acquisitions, even by the same sensor, can create further complications that go beyond wavelength: The C-band Sentinel-1 SAR images land areas in VH and VV mode, whereas it switches to HH and HV polarizations when over oceans (this is driven by the scientific and operational users need to map sea ice, which is better detectable in these modes). DOFA also does not demonstrably test what we consider to be this framework’s most interesting potential capability: the capacity to operate effectively on downstream tasks that rely on a sensor not found in the training dataset.

SeCo [64] and GASSL [3] demonstrated the value of utilizing temporal data in training, but cautioned that the learned representations were agnostic to seasonal changes. The seasonal contrastive objective could be helpful as an additional task, when taken into account with other pre-training tasks that take seasonal change into account. Ultimately, multi-task training on complementary tasks, such as this particular example, is somewhat costly, but it results in representations that learn the unique features inherent to each task while avoiding the problem of overfitting.

Aside from the SeCo objective, SatMAE’s [22] breakthrough in adding temporal information to the positional encoding of images could serve as a useful way to introduce temporal information into existing methods. However, caution should be taken to ensure that such encoders are robust enough to not be overly reliant on temporal information. ScaleMAE’s [74] novel approach of normalizing positional embeddings to account for image scale also seems to be a methodology that could be easily applied to other models within the field, presuming those models utilize a ViT framework.

8 Conclusion

In this paper we presented on a variety of SSL approaches currently utilized in RS foundation models and traced these approaches back to their origins in the CV field to develop a better understanding of the current swathe of RS foundation models and potential paths for future development. We examined:

- (1) Prospective options for lowering compute costs for training RS foundation models.
- (2) Varying benefits and drawbacks of RS embeddings learned with different frameworks and SSL tasks.
- (3) Inherent opportunities available for leveraging multi-sensory Earth observations to train RS foundation models on publicly available unlabeled data.

Acknowledgments

To the GeoHAI lab, for all of their ideas, support, and kindness.

References

- [1] Suleiman O. Alswiss, Zorana Jelenak, Paul S. Chang, Jun Dong Park, and Patrick Meyers. 2015. Inter-calibration Results of the Advanced Microwave Scanning Radiometer-2 Over Ocean. *IEEE Journal of Selected Topics in Applied Earth Observations and Remote Sensing* 8, 9 (Sept. 2015), 4230–4238. doi:10.1109/JSTARS.2014.2330980 Conference Name: IEEE Journal of Selected Topics in Applied Earth Observations and Remote Sensing.
- [2] Neal T. Anderson and Giovanni B. Marchisio. 2012. WorldView-2 and the evolution of the DigitalGlobe remote sensing satellite constellation: introductory paper for the special session on WorldView-2. In *Algorithms and Technologies for Multispectral, Hyperspectral, and Ultraspectral Imagery XVIII*, Vol. 8390. SPIE, 166–180. doi:10.1117/12.919756
- [3] Kumar Ayush, Burak Uzkent, Chenlin Meng, Kumar Tanmay, Marshall Burke, David Lobell, and Stefano Ermon. 2021. Geography-Aware Self-Supervised Learning. 10181–10190. https://openaccess.thecvf.com/content/ICCV2021/html/Ayush_Geography-Aware_Self-Supervised_Learning_ICCV_2021_paper.html
- [4] Michael Bailey, Rachel Cao, Theresa Kuchler, Johannes Stroebel, and Arlene Wong. 2018. Social connectedness: Measurement, determinants, and effects. *Journal of Economic Perspectives* 32, 3 (2018), 259–280.
- [5] Jan Barowski, Jochen Jebramcik, Jonas Wagner, Nils Pohl, and Ilona Rolfes. 2019. Spatial Identification of Dielectric Properties using Synthetic Aperture Radar. In *2019 IEEE MTT-S International Microwave Workshop Series on Advanced Materials and Processes for RF and THz Applications (IMWS-AMP)*. 139–141. doi:10.1109/IMWS-AMP.2019.8880121
- [6] Christopher F. Brown, Steven P. Brumby, Brookie Guzder-Williams, Tanya Birch, Samantha Brooks Hyde, Joseph Mazzariello, Wanda Czerwinski, Valerie J. Pasquarella, Robert Haertel, Simon Ilyushchenko, Kurt Schwehr, Mikaela Weisse, Fred Stolle, Craig Hanson, Oliver Guinan, Rebecca Moore, and Alexander M. Tait. 2022. Dynamic World, Near real-time global 10 m land use land cover mapping. *Scientific Data* 9, 1 (June 2022), 251. doi:10.1038/s41597-022-01307-4
- [7] William M. Brown and Leonard J. Porcello. 1969. An introduction to synthetic-aperture radar. *IEEE Spectrum* 6, 9 (Sept. 1969), 52–62. doi:10.1109/MSPEC.1969.5213674 Conference Name: IEEE Spectrum.
- [8] John Canny. 1986. A Computational Approach to Edge Detection. *IEEE Transactions on Pattern Analysis and Machine Intelligence* PAMI-8, 6 (Nov. 1986), 679–698. doi:10.1109/TPAMI.1986.4767851 Conference Name: IEEE Transactions on Pattern Analysis and Machine Intelligence.
- [9] Mathilde Caron, Hugo Touvron, Ishan Misra, Hervé Jégou, Julien Mairal, Piotr Bojanowski, and Armand Joulin. 2021. Emerging Properties in Self-Supervised Vision Transformers. doi:10.48550/arXiv.2104.14294 arXiv:2104.14294 [cs].
- [10] Davide Castelletti, Gordon Farquharson, Craig Stringham, Michael Duersch, and Duncan Eddy. 2021. Capella Space First Operational SAR Satellite. In *2021 IEEE International Geoscience and Remote Sensing Symposium IGARSS*. 1483–1486. doi:10.1109/IGARSS47720.2021.9554100 ISSN: 2153-7003.
- [11] Vicente Vivanco Cepeda, Gaurav Kumar Nayak, and Mubarak Shah. 2023. GeoCLIP: Clip-Inspired Alignment between Locations and Images for Effective Worldwide Geo-localization. <http://arxiv.org/abs/2309.16020> arXiv:2309.16020 [cs].

- [12] Bruce Chapman and Paul Rosen. 2024. Overview of NASA’S calibration and validation activities for the NISAR mission. In *EUSAR 2024; 15th European Conference on Synthetic Aperture Radar*. 1101–1103. <https://ieeexplore.ieee.org/abstract/document/10659495>
- [13] Vinod Kumar Chauhan, Jiandong Zhou, Ping Lu, Soheila Molaei, and David A. Clifton. 2024. A brief review of hypernetworks in deep learning. *Artificial Intelligence Review* 57, 9 (Sept. 2024), 1–29. doi:10.1007/s10462-024-10862-8 Company: Springer Distributor: Springer Institution: Springer Label: Springer Number: 9 Publisher: Springer Netherlands.
- [14] Ting Chen, Simon Kornblith, Mohammad Norouzi, and Geoffrey Hinton. 2020. A Simple Framework for Contrastive Learning of Visual Representations. <http://arxiv.org/abs/2002.05709> arXiv:2002.05709 [cs, stat].
- [15] Xinlei Chen and Kaiming He. 2021. Exploring Simple Siamese Representation Learning. 15750–15758. https://openaccess.thecvf.com/content/CVPR2021/html/Chen_Exploring_Simple_Siamese_Representation_Learning_CVPR_2021_paper.html
- [16] Yile Chen, Weiming Huang, Kaiqi Zhao, Yue Jiang, and Gao Cong. 2024. Self-supervised Learning for Geospatial AI: A Survey. doi:10.48550/arXiv.2408.12133 arXiv:2408.12133 [cs].
- [17] Y. Chen, X. S. Yu, and K. Qin. 2023. MMCP: A MULTI-MODAL CONTRASTIVE PRE-TRAINING MODEL FOR PLACE REPRESENTATION BASED ON THE SPATIO-TEMPORAL FRAMEWORK. *ISPRS Annals of the Photogrammetry, Remote Sensing and Spatial Information Sciences* X-1-W1-2023 (Dec. 2023), 303–310. doi:10.5194/isprs-annals-X-1-W1-2023-303-2023 Conference Name: ISPRS Geospatial Week 2023 - 2–7 September 2023, Cairo, Egypt Publisher: Copernicus GmbH.
- [18] Gong Cheng, Junwei Han, and Xiaoqiang Lu. 2017. Remote Sensing Image Scene Classification: Benchmark and State of the Art. *Proc. IEEE* 105, 10 (Oct. 2017), 1865–1883. doi:10.1109/JPROC.2017.2675998 Conference Name: Proceedings of the IEEE.
- [19] Gordon Christie, Neil Fendley, James Wilson, and Ryan Mukherjee. 2018. Functional Map of the World. 6172–6180. https://openaccess.thecvf.com/content_cvpr_2018/html/Christie_Functional_Map_of_CVPR_2018_paper.html
- [20] Carmen Cillero Castro, Jose Antonio Domínguez Gómez, Jordi Delgado Martín, Boris Alejandro Hinojo Sánchez, Jose Luis Cereijo Arango, Federico Andrés Cheda Tuya, and Ramon Díaz-Varela. 2020. An UAV and Satellite Multispectral Data Approach to Monitor Water Quality in Small Reservoirs. *Remote Sensing* 12, 9 (Jan. 2020), 1514. doi:10.3390/rs12091514 Number: 9 Publisher: Multidisciplinary Digital Publishing Institute.
- [21] Martin Claverie, Junchang Ju, Jeffrey G. Masek, Jennifer L. Dungan, Eric F. Vermote, Jean-Claude Roger, Sergii V. Skakun, and Christopher Justice. 2018. The Harmonized Landsat and Sentinel-2 surface reflectance data set. *Remote Sensing of Environment* 219 (Dec. 2018), 145–161. doi:10.1016/j.rse.2018.09.002
- [22] Yezhen Cong, Samar Khanna, Chenlin Meng, Patrick Liu, Erik Rozi, Yutong He, Marshall Burke, David B. Lobell, and Stefano Ermon. 2023. SatMAE: Pre-training Transformers for Temporal and Multi-Spectral Satellite Imagery. doi:10.48550/arXiv.2207.08051 arXiv:2207.08051 [cs].
- [23] N. Dalal and B. Triggs. 2005. Histograms of oriented gradients for human detection. In *2005 IEEE Computer Society Conference on Computer Vision and Pattern Recognition (CVPR’05)*, Vol. 1. 886–893 vol. 1. doi:10.1109/CVPR.2005.177 ISSN: 1063-6919.
- [24] Rodrigo Caye Daudt, Bertr Le Saux, Alexandre Boulch, and Yann Gousseau. 2018. Urban Change Detection for Multispectral Earth Observation Using Convolutional Neural Networks. In *IGARSS 2018 - 2018 IEEE International Geoscience and Remote Sensing Symposium*. 2115–2118. doi:10.1109/IGARSS.2018.8518015 ISSN: 2153-7003.
- [25] Mostafa Dehghani, Josip Djolonga, Basil Mustafa, Piotr Padlewski, Jonathan Heek, Justin Gilmer, Andreas Steiner, Mathilde Caron, Robert Geirhos, Ibrahim Alabdulmohsin, Rodolphe Jenatton, Lucas Beyer, Michael Tschannen, Anurag Arnab, Xiao Wang, Carlos Riquelme, Matthias Minderer, Joan Puigcerver, Utku Evci, Manoj Kumar, Sjoerd van Steenkiste, Gamaleldin F. Elsayed, Aravindh Mahendran, Fisher Yu, Avital Oliver, Fantine Huot, Jasmijn Bastings, Mark Patrick Collier, Alexey Gritsenko, Vignesh Birodkar, Cristina Vasconcelos, Yi Tay, Thomas Mensink, Alexander Kolesnikov, Filip Pavetić, Dustin Tran, Thomas Kipf, Mario Lučić, Xiaohua Zhai, Daniel Keysers, Jeremiah Harmsen, and Neil Houlsby. 2023. Scaling Vision Transformers to 22 Billion Parameters. doi:10.48550/arXiv.2302.05442 arXiv:2302.05442 [cs].
- [26] Dara Entekhabi, Eni G. Njoku, Peggy E. O’Neill, Kent H. Kellogg, Wade T. Crow, Wendy N. Edelstein, Jared K. Entin, Shawn D. Goodman, Thomas J. Jackson, Joel Johnson, John Kimball, Jeffrey R. Piepmeier, Randal D. Koster, Neil Martin, Kyle C. McDonald, Mahta Moghaddam, Susan Moran, Rolf Reichle, J. C. Shi, Michael W. Spencer, Samuel W. Thurman, Leung Tsang, and Jakob Van Zyl. 2010. The Soil Moisture Active Passive (SMAP) Mission. *Proc. IEEE* 98, 5 (May 2010), 704–716. doi:10.1109/JPROC.2010.2043918 Conference Name: Proceedings of the IEEE.
- [27] Christoph Feichtenhofer, Haoqi Fan, Yanghao Li, and Kaiming He. 2022. Masked Autoencoders As Spatiotemporal Learners. *Advances in Neural Information Processing Systems* 35 (Dec. 2022), 35946–35958. https://proceedings.neurips.cc/paper_files/paper/2022/hash/e97d1081481a4017df96b51be31001d3-Abstract-Conference.html
- [28] Anthony Fuller, Koreen Millard, and James R. Green. 2023. CROMA: Remote Sensing Representations with Contrastive Radar-Optical Masked Autoencoders. doi:10.48550/arXiv.2311.00566 arXiv:2311.00566 [cs].
- [29] Guangshuai Gao, Qingjie Liu, and Yunhong Wang. 2021. Counting From Sky: A Large-Scale Data Set for Remote Sensing Object Counting and a Benchmark Method. *IEEE Transactions on Geoscience and Remote Sensing* 59, 5 (May 2021), 3642–3655. doi:10.1109/TGRS.2020.3020555 Conference Name: IEEE Transactions on Geoscience and Remote Sensing.
- [30] Tianyu Gao, Xingcheng Yao, and Danqi Chen. 2022. SimCSE: Simple Contrastive Learning of Sentence Embeddings. doi:10.48550/arXiv.2104.08821 arXiv:2104.08821 [cs].
- [31] Jean-Bastien Grill, Florian Strub, Florent Altché, Corentin Tallec, Pierre H. Richemond, Elena Buchatskaya, Carl Doersch, Bernardo Avila Pires, Zhaohan Daniel Guo, Mohammad Gheshlaghi Azar, Bilal Piot, Koray Kavukcuoglu, Rémi Munos, and Michal Valko. 2020. Bootstrap your own latent: A new approach to self-supervised Learning. doi:10.48550/arXiv.2006.07733 arXiv:2006.07733 [cs, stat].

- [32] Dipanwita Haldar, Anup Das, Shiv Mohan, Om Pal, Ramesh S. Hooda, and Manab Chakraborty. 2012. ASSESSMENT OF L-BAND SAR DATA AT DIFFERENT POLARIZATION COMBINATIONS FOR CROP AND OTHER LANDUSE CLASSIFICATION. *Progress In Electromagnetics Research B* 36 (2012), 303–321. doi:10.2528/PIERB11071106
- [33] Kaiming He, Xinlei Chen, Saining Xie, Yanghao Li, Piotr Dollár, and Ross Girshick. 2021. Masked Autoencoders Are Scalable Vision Learners. doi:10.48550/arXiv.2111.06377 arXiv:2111.06377 [cs].
- [34] Kaiming He, Haoqi Fan, Yuxin Wu, Saining Xie, and Ross Girshick. 2020. Momentum Contrast for Unsupervised Visual Representation Learning. 9729–9738. https://openaccess.thecvf.com/content_CVPR_2020/html/He_Momentum_Contrast_for_Unsupervised_Visual_Representation_Learning_CVPR_2020_paper.html
- [35] Kaiming He, Xiangyu Zhang, Shaoqing Ren, and Jian Sun. 2015. Deep Residual Learning for Image Recognition. doi:10.48550/arXiv.1512.03385 arXiv:1512.03385 [cs].
- [36] Patrick Helber, Benjamin Bischke, Andreas Dengel, and Damian Borth. 2019. EuroSAT: A Novel Dataset and Deep Learning Benchmark for Land Use and Land Cover Classification. doi:10.48550/arXiv.1709.00029 arXiv:1709.00029 version: 2.
- [37] D. H. Hoekman and B. A. M. Bouman. 1993. Interpretation of C- and X-band radar images over an agricultural area, the Flevoland test site in the Agriscatt-87 campaign. *International Journal of Remote Sensing* 14, 8 (May 1993), 1577–1594. doi:10.1080/01431169308953987
- [38] Yujun Hou, Matias Quintana, Maxim Khomiakov, Winston Yap, Jiani Ouyang, Koichi Ito, Zeyu Wang, Tianhong Zhao, and Filip Biljecki. 2024. Global Streetscapes — A comprehensive dataset of 10 million street-level images across 688 cities for urban science and analytics. *ISPRS Journal of Photogrammetry and Remote Sensing* 215 (Sept. 2024), 216–238. doi:10.1016/j.isprsjprs.2024.06.023
- [39] Sha Huang, Lina Tang, Joseph P. Hupy, Yang Wang, and Guofan Shao. 2021. A commentary review on the use of normalized difference vegetation index (NDVI) in the era of popular remote sensing. *Journal of Forestry Research* 32, 1 (Feb. 2021), 1–6. doi:10.1007/s11676-020-01155-1
- [40] Vladimir Ignatenko, Pekka Laurila, Andrea Radius, Leszek Lamentowski, Oleg Antropov, and Darren Muff. 2020. ICEYE Microsatellite SAR Constellation Status Update: Evaluation of First Commercial Imaging Modes. In *IGARSS 2020 - 2020 IEEE International Geoscience and Remote Sensing Symposium*. 3581–3584. doi:10.1109/IGARSS39084.2020.9324531 ISSN: 2153-7003.
- [41] Pallavi Jain, Bianca Schoen-Phelan, and Robert Ross. 2022. Self-Supervised Learning for Invariant Representations from Multi-Spectral and SAR Images. *IEEE Journal of Selected Topics in Applied Earth Observations and Remote Sensing* 15 (2022), 7797–7808. doi:10.1109/JSTARS.2022.3204888 arXiv:2205.02049 [cs].
- [42] Umangi Jain, Alex Wilson, and Varun Gulshan. 2022. Multimodal contrastive learning for remote sensing tasks. <http://arxiv.org/abs/2209.02329> arXiv:2209.02329 [cs].
- [43] Johannes Jakubik, Sujit Roy, C. E. Phillips, Paolo Fraccaro, Denys Godwin, Bianca Zadrozny, Daniela Szwarcman, Carlos Gomes, Gabby Nyirjesy, Blair Edwards, Daiki Kimura, Naomi Simumba, Linsong Chu, S. Karthik Mukkavilli, Devyani Lambhate, Kamal Das, Ranjini Bangalore, Dario Oliveira, Michal Muszynski, Kumar Ankur, Muthukumaran Ramasubramanian, Iksha Gurung, Sam Khallaghi, Hanxi, Li, Michael Cecil, Maryam Ahmadi, Fatemeh Kordi, Hamed Alemohammad, Manil Maskey, Raghu Ganti, Kommy Weldemariam, and Rahul Ramachandran. 2023. Foundation Models for Generalist Geospatial Artificial Intelligence. <http://arxiv.org/abs/2310.18660> arXiv:2310.18660 [cs].
- [44] Sepideh Jalayer, Samira Alkaee Taleghan, Rafael Pires de Lima, Behzad Vahedi, Nick Hughes, Farnoush Banaei-Kashani, and Morteza Karimzadeh. 2025. Enhancing and Interpreting Deep Learning for Sea Ice Charting using the AutoICE Benchmark. *Remote Sensing Applications: Society and Environment* (2025), 101538.
- [45] Chao Jia, Yinfei Yang, Ye Xia, Yi-Ting Chen, Zarana Parekh, Hieu Pham, Quoc V. Le, Yunhsuan Sung, Zhen Li, and Tom Duerig. 2021. Scaling Up Visual and Vision-Language Representation Learning With Noisy Text Supervision. doi:10.48550/arXiv.2102.05918 arXiv:2102.05918 [cs].
- [46] Li Jing, Pascal Vincent, Yann LeCun, and Yuandong Tian. 2022. Understanding Dimensional Collapse in Contrastive Self-supervised Learning. doi:10.48550/arXiv.2110.09348 arXiv:2110.09348.
- [47] C. O Justice, J. R. G Townshend, E. F Vermote, E Masuoka, R. E Wolfe, N Saleous, D. P Roy, and J. T Morissette. 2002. An overview of MODIS Land data processing and product status. *Remote Sensing of Environment* 83, 1 (Nov. 2002), 3–15. doi:10.1016/S0034-4257(02)00084-6
- [48] Konstantin Klemmer, Esther Rolf, Caleb Robinson, Lester Mackey, and Marc Rußwurm. 2024. SatCLIP: Global, General-Purpose Location Embeddings with Satellite Imagery. doi:10.48550/arXiv.2311.17179 arXiv:2311.17179 [cs].
- [49] M. V. Koroteev. 2021. BERT: A Review of Applications in Natural Language Processing and Understanding. doi:10.48550/arXiv.2103.11943 arXiv:2103.11943 [cs].
- [50] Gerhard Krieger, Alberto Moreira, Hauke Fiedler, Irena Hajnsek, Marian Werner, Marwan Younis, and Manfred Zink. 2007. TanDEM-X: A Satellite Formation for High-Resolution SAR Interferometry. *IEEE Transactions on Geoscience and Remote Sensing* 45, 11 (Nov. 2007), 3317–3341. doi:10.1109/TGRS.2007.900693
- [51] Alexandre Lacoste, Nils Lehmann, Pau Rodriguez, Evan David Sherwin, Hannah Kerner, Björn Lütjens, Jeremy Andrew Irvin, David Dao, Hamed Alemohammad, Alexandre Drouin, Mehmet Gunturkun, Gabriel Huang, David Vazquez, Dava Newman, Yoshua Bengio, Stefano Ermon, and Xiao Xiang Zhu. 2023. GEO-Bench: Toward Foundation Models for Earth Monitoring. <http://arxiv.org/abs/2306.03831> arXiv:2306.03831 [cs].
- [52] Liunian Harold Li, Mark Yatskar, Da Yin, Cho-Jui Hsieh, and Kai-Wei Chang. 2019. VisualBERT: A Simple and Performant Baseline for Vision and Language. doi:10.48550/arXiv.1908.03557 arXiv:1908.03557 [cs].
- [53] Xuyang Li, Danfeng Hong, and Jocelyn Chanussot. 2024. S2MAE: A Spatial-Spectral Pretraining Foundation Model for Spectral Remote Sensing Data. In *2024 IEEE/CVF Conference on Computer Vision and Pattern Recognition (CVPR)*. IEEE, Seattle, WA, USA, 27696–27705. doi:10.1109/CVPR52733.2024.02616

- [54] Zhihao Li, Biao Hou, Siteng Ma, Zitong Wu, Xianpeng Guo, Bo Ren, and Licheng Jiao. 2024. Masked Angle-Aware Autoencoder for Remote Sensing Images. [doi:10.48550/arXiv.2408.01946](https://arxiv.org/abs/2408.01946) arXiv:2408.01946 [cs].
- [55] Fan Liu, Delong Chen, Zhangqingyun Guan, Xiaocong Zhou, Jiale Zhu, Qiaolin Ye, Liyong Fu, and Jun Zhou. 2024. RemoteCLIP: A Vision Language Foundation Model for Remote Sensing. *IEEE Transactions on Geoscience and Remote Sensing* 62 (2024), 1–16. [doi:10.1109/TGRS.2024.3390838](https://doi.org/10.1109/TGRS.2024.3390838) Conference Name: IEEE Transactions on Geoscience and Remote Sensing.
- [56] Zeping Liu, Fan Zhang, Junfeng Jiao, Ni Lao, and Gengchen Mai. 2025. GAIR: Improving Multimodal Geo-Foundation Model with Geo-Aligned Implicit Representations. [doi:10.48550/arXiv.2503.16683](https://arxiv.org/abs/2503.16683) arXiv:2503.16683 [cs].
- [57] Yang Long, Gui-Song Xia, Shengyang Li, Wen Yang, Michael Ying Yang, Xiao Xiang Zhu, Liangpei Zhang, and Deren Li. 2021. On Creating Benchmark Dataset for Aerial Image Interpretation: Reviews, Guidances, and Million-AID. *IEEE Journal of Selected Topics in Applied Earth Observations and Remote Sensing* 14 (2021), 4205–4230. [doi:10.1109/JSTARS.2021.3070368](https://doi.org/10.1109/JSTARS.2021.3070368) Conference Name: IEEE Journal of Selected Topics in Applied Earth Observations and Remote Sensing.
- [58] David G. Lowe. 2004. Distinctive Image Features from Scale-Invariant Keypoints. *International Journal of Computer Vision* 60, 2 (Nov. 2004), 91–110. [doi:10.1023/B:VISI.0000029664.99615.94](https://doi.org/10.1023/B:VISI.0000029664.99615.94)
- [59] Jiasen Lu, Dhruv Batra, Devi Parikh, and Stefan Lee. 2019. ViLBERT: Pretraining Task-Agnostic Visiolinguistic Representations for Vision-and-Language Tasks. In *Advances in Neural Information Processing Systems*, Vol. 32. Curran Associates, Inc. https://proceedings.neurips.cc/paper_files/paper/2019/hash/c74d97b01eae257e44aa9d5bade97baf-Abstract.html
- [60] Siqi Lu, Junlin Guo, James R. Zimmer-Dauphinee, Jordan M. Nieuwsma, Xiao Wang, Parker VanValkenburgh, Steven A. Wernke, and Yuankai Huo. 2025. Vision Foundation Models in Remote Sensing: A Survey. [doi:10.48550/arXiv.2408.03464](https://arxiv.org/abs/2408.03464) arXiv:2408.03464 [cs].
- [61] Ahmed Mahmood. 2014. RADARSAT-1 Background Mission Implementation and Accomplishments. *Canadian Journal of Remote Sensing* 40, 6 (Nov. 2014), 385–395. [doi:10.1080/07038992.2014.999913](https://doi.org/10.1080/07038992.2014.999913) Publisher: Canadian Aeronautics and Space Institute _eprint: <https://doi.org/10.1080/07038992.2014.999913>.
- [62] Gengchen Mai, Weiming Huang, Jin Sun, Suhang Song, Deepak Mishra, Ninghao Liu, Song Gao, Tianming Liu, Gao Cong, Yingjie Hu, Chris Cundy, Ziyuan Li, Rui Zhu, and Ni Lao. 2023. On the Opportunities and Challenges of Foundation Models for Geospatial Artificial Intelligence. [doi:10.48550/arXiv.2304.06798](https://arxiv.org/abs/2304.06798) arXiv:2304.06798 [cs].
- [63] Gengchen Mai, Ni Lao, Yutong He, Jiaming Song, and Stefano Ermon. 2023. CSP: Self-Supervised Contrastive Spatial Pre-Training for Geospatial-Visual Representations. [http://arxiv.org/abs/2305.01118](https://arxiv.org/abs/2305.01118) arXiv:2305.01118.
- [64] Oscar Mañas, Alexandre Lacoste, Xavier Giro-i Nieto, David Vazquez, and Pau Rodriguez. 2021. Seasonal Contrast: Unsupervised Pre-Training from Uncurated Remote Sensing Data. [doi:10.48550/arXiv.2103.16607](https://arxiv.org/abs/2103.16607) arXiv:2103.16607 [cs].
- [65] L C Morena, James , K V , and J. Beck. 2004. An introduction to the RADARSAT-2 mission. *Canadian Journal of Remote Sensing* 30, 3 (Jan. 2004), 221–234. [doi:10.5589/m04-004](https://doi.org/10.5589/m04-004) Publisher: Canadian Aeronautics and Space Institute _eprint: <https://doi.org/10.5589/m04-004>.
- [66] S. Joseph Munchak, Sarah Ringerud, Ludovic Brucker, Yalei You, Iris de Gelis, and Catherine Prigent. 2020. An Active–Passive Microwave Land Surface Database From GPM. *IEEE Transactions on Geoscience and Remote Sensing* 58, 9 (Sept. 2020), 6224–6242. [doi:10.1109/TGRS.2020.2975477](https://doi.org/10.1109/TGRS.2020.2975477) Conference Name: IEEE Transactions on Geoscience and Remote Sensing.
- [67] Vishal Nedungadi, Ankit Kariyaa, Stefan Oehmcke, Serge Belongie, Christian Igel, and Nico Lang. 2024. MMEarth: Exploring Multi-Modal Pretext Tasks For Geospatial Representation Learning. [http://arxiv.org/abs/2405.02771](https://arxiv.org/abs/2405.02771) arXiv:2405.02771 [cs].
- [68] Elnaz Neinavaz, Martin Schlerf, Roshanak Darvishzadeh, Max Gerhards, and Andrew K. Skidmore. 2021. Thermal infrared remote sensing of vegetation: Current status and perspectives. *International Journal of Applied Earth Observation and Geoinformation* 102 (Oct. 2021), 102415. [doi:10.1016/j.jag.2021.102415](https://doi.org/10.1016/j.jag.2021.102415)
- [69] OpenAI, Josh Achiam, Steven Adler, Sandhini Agarwal, Lama Ahmad, Ilge Akkaya, Florencia Leoni Aleman, Diogo Almeida, Janko Altenschmidt, Sam Altman, Shyamal Anadkat, Red Avila, Igor Babuschkin, Suchir Balaji, Valerie Balcom, Paul Baltescu, Haiming Bao, Mohammad Bavarian, Jeff Belgum, Irwan Bello, Jake Berdine, Gabriel Bernadett-Shapiro, Christopher Berner, Lenny Bogdonoff, Oleg Boiko, Madelaine Boyd, Anna-Luisa Brakman, Greg Brockman, Tim Brooks, Miles Brundage, Kevin Button, Trevor Cai, Rosie Campbell, Andrew Cann, Brittany Carey, Chelsea Carlson, Rory Carmichael, Brooke Chan, Che Chang, Fotis Chantzis, Derek Chen, Sully Chen, Ruby Chen, Jason Chen, Mark Chen, Ben Chess, Chester Cho, Casey Chu, Hyung Won Chung, Dave Cummings, Jeremiah Currier, Yunxing Dai, Cory Decareaux, Thomas Degry, Noah Deutsch, Damien Deville, Arka Dhar, David Dohan, Steve Dowling, Sheila Dunning, Adrien Ecoffet, Atty Eleti, Tyna Eloundou, David Farhi, Liam Fedus, Niko Felix, Simón Posada Fishman, Juston Forte, Isabella Fulford, Leo Gao, Elie Georges, Christian Gibson, Vik Goel, Tarun Gogineni, Gabriel Goh, Rapha Gontijo-Lopes, Jonathan Gordon, Morgan Grafstein, Scott Gray, Ryan Greene, Joshua Gross, Shixiang Shane Gu, Yufei Guo, Chris Hallacy, Jesse Han, Jeff Harris, Yuchen He, Mike Heaton, Johannes Heidecke, Chris Hesse, Alan Hickey, Wade Hickey, Peter Hoeschele, Brandon Houghton, Kenny Hsu, Shengli Hu, Xin Hu, Joost Huizinga, Shantanu Jain, Shawn Jain, Joanne Jang, Angela Jiang, Roger Jiang, Haozhun Jin, Denny Jin, Shino Jomoto, Billie Jonn, Heewoo Jun, Tomer Kaftan, Łukasz Kaiser, Ali Kamali, Ingmar Kanitscheider, Nitish Shirish Keskar, Tabarak Khan, Logan Kilpatrick, Jong Wook Kim, Christina Kim, Yongjik Kim, Jan Hendrik Kirchner, Jamie Kiros, Matt Knight, Daniel Kokotajlo, Łukasz Kondraciuk, Andrew Kondrich, Aris Konstantinidis, Kyle Kopic, Gretchen Krueger, Vishal Kuo, Michael Lampe, Ikai Lan, Teddy Lee, Jan Leike, Jade Leung, Daniel Levy, Chak Ming Li, Rachel Lim, Stephanie Lin, Mateusz Litwin, Theresa Lopez, Ryan Lowe, Patricia Lue, Anna Makanju, Kim Malfacini, Sam Manning, Todor Markov, Yaniv Markovski, Bianca Martin, Katie Mayer, Andrew Mayne, Bob McGrew, Scott Mayer McKinney, Christine McLeavey, Paul McMillan, Jake McNeil, David Medina, Aalok Mehta, Jacob Menick, Luke Metz, Andrey Mishchenko, Pamela Mishkin, Vinnie Monaco, Evan Morikawa, Daniel Mossing, Tong Mu, Mira Murati, Oleg Murk, David Mély, Ashvin Nair, Reiichiro Nakano, Rajeev Nayak,

- Arvind Neelakantan, Richard Ngo, Hyeonwoo Noh, Long Ouyang, Cullen O’Keefe, Jakub Pachocki, Alex Paino, Joe Palermo, Ashley Pantuliano, Giambattista Parascandolo, Joel Parish, Emy Parparita, Alex Passos, Mikhail Pavlov, Andrew Peng, Adam Perelman, Filipe de Avila Belbute Peres, Michael Petrov, Henrique Ponde de Oliveira Pinto, Michael, Pokorny, Michelle Pokrass, Vitchyr H. Pong, Tolly Powell, Alethea Power, Boris Power, Elizabeth Proehl, Raul Puri, Alec Radford, Jack Rae, Aditya Ramesh, Cameron Raymond, Francis Real, Kendra Rimbach, Carl Ross, Bob Rotsted, Henri Roussez, Nick Ryder, Mario Saltarelli, Ted Sanders, Shibani Santurkar, Girish Sastry, Heather Schmidt, David Schnurr, John Schulman, Daniel Selsam, Kyla Sheppard, Toki Sherbakov, Jessica Shieh, Sarah Shoker, Pranav Shyam, Szymon Sidor, Eric Sigler, Maddie Simens, Jordan Sitkin, Katarina Slama, Ian Sohl, Benjamin Sokolowsky, Yang Song, Natalie Staudacher, Felipe Petroski Such, Natalie Summers, Ilya Sutskever, Jie Tang, Nikolas Tezak, Madeleine B. Thompson, Phil Tillet, Amin Tootoonchian, Elizabeth Tseng, Preston Tuggle, Nick Turley, Jerry Tworek, Juan Felipe Cerón Uribe, Andrea Vallone, Arun Vijayvergiya, Chelsea Voss, Carroll Wainwright, Justin Jay Wang, Alvin Wang, Ben Wang, Jonathan Ward, Jason Wei, C. J. Weinmann, Akila Welihinda, Peter Welinder, Jiayi Weng, Lilian Weng, Matt Wiethoff, Dave Willner, Clemens Winter, Samuel Wolrich, Hannah Wong, Lauren Workman, Sherwin Wu, Jeff Wu, Michael Wu, Kai Xiao, Tao Xu, Sarah Yoo, Kevin Yu, Qiming Yuan, Wojciech Zaremba, Rowan Zellers, Chong Zhang, Marvin Zhang, Shengjia Zhao, Tianhao Zheng, Juntang Zhuang, William Zhuk, and Barret Zoph. 2024. GPT-4 Technical Report. [doi:10.48550/arXiv.2303.08774](https://arxiv.org/abs/2303.08774) arXiv:2303.08774 [cs].
- [70] Rafael Pires de Lima, Behzad Vahedi, Nick Hughes, Andrew P Barrett, Walter Meier, and Morteza Karimzadeh. 2023. Enhancing sea ice segmentation in Sentinel-1 images with atrous convolutions. *International Journal of Remote Sensing* 44, 17 (2023), 5344–5374.
- [71] Dimitris Poursanidis, Dimosthenis Traganos, Peter Reinartz, and Nektarios Chrysoulakis. 2019. On the use of Sentinel-2 for coastal habitat mapping and satellite-derived bathymetry estimation using downscaled coastal aerosol band. *International Journal of Applied Earth Observation and Geoinformation* 80 (Aug. 2019), 58–70. [doi:10.1016/j.jag.2019.03.012](https://doi.org/10.1016/j.jag.2019.03.012)
- [72] Ofir Press, Noah A. Smith, and Mike Lewis. 2022. Train Short, Test Long: Attention with Linear Biases Enables Input Length Extrapolation. [doi:10.48550/arXiv.2108.12409](https://arxiv.org/abs/2108.12409) arXiv:2108.12409 [cs].
- [73] Alec Radford, Jong Wook Kim, Chris Hallacy, Aditya Ramesh, Gabriel Goh, Sandhini Agarwal, Girish Sastry, Amanda Askell, Pamela Mishkin, Jack Clark, Gretchen Krueger, and Ilya Sutskever. 2021. Learning Transferable Visual Models From Natural Language Supervision. [http://arxiv.org/abs/2103.00020](https://arxiv.org/abs/2103.00020) arXiv:2103.00020 [cs].
- [74] Colorado J. Reed, Ritwik Gupta, Shufan Li, Sarah Brockman, Christopher Funk, Brian Clipp, Kurt Keutzer, Salvatore Candido, Matt Uyttendaele, and Trevor Darrell. 2023. Scale-MAE: A Scale-Aware Masked Autoencoder for Multiscale Geospatial Representation Learning. [doi:10.48550/arXiv.2212.14532](https://arxiv.org/abs/2212.14532) arXiv:2212.14532 [cs].
- [75] Esther Rolf, Konstantin Klemmer, Caleb Robinson, and Hannah Kerner. 2024. Mission Critical – Satellite Data is a Distinct Modality in Machine Learning. [doi:10.48550/arXiv.2402.01444](https://arxiv.org/abs/2402.01444) arXiv:2402.01444 [cs].
- [76] Esther Rolf, Jonathan Proctor, Tamma Carleton, Ian Bolliger, Vaishaal Shankar, Miyabi Ishihara, Benjamin Recht, and Solomon Hsiang. 2021. A generalizable and accessible approach to machine learning with global satellite imagery. *Nature Communications* 12, 1 (July 2021), 4392. [doi:10.1038/s41467-021-24638-z](https://doi.org/10.1038/s41467-021-24638-z)
- [77] Ake Rosenqvist, Masanobu Shimada, Norimasa Ito, and Manabu Watanabe. 2007. ALOS PALSAR: A Pathfinder Mission for Global-Scale Monitoring of the Environment. *IEEE Transactions on Geoscience and Remote Sensing* 45, 11 (Nov. 2007), 3307–3316. [doi:10.1109/TGRS.2007.901027](https://doi.org/10.1109/TGRS.2007.901027) Conference Name: IEEE Transactions on Geoscience and Remote Sensing.
- [78] Olga Russakovsky, Jia Deng, Hao Su, Jonathan Krause, Sanjeev Satheesh, Sean Ma, Zhiheng Huang, Andrej Karpathy, Aditya Khosla, Michael Bernstein, Alexander C. Berg, and Li Fei-Fei. 2015. ImageNet Large Scale Visual Recognition Challenge. *International Journal of Computer Vision* 115, 3 (Dec. 2015), 211–252. [doi:10.1007/s11263-015-0816-y](https://doi.org/10.1007/s11263-015-0816-y)
- [79] Marc Rußwurm, Konstantin Klemmer, Esther Rolf, Robin Zbinden, and Devis Tuia. 2023. Geographic location encoding with spherical harmonics and sinusoidal representation networks. *arXiv preprint arXiv:2310.06743* (2023).
- [80] Amanpreet Singh, Ronghang Hu, Vedanuj Goswami, Guillaume Couairon, Wojciech Galuba, Marcus Rohrbach, and Douwe Kiela. 2022. FLAVA: A Foundational Language And Vision Alignment Model. In *2022 IEEE/CVF Conference on Computer Vision and Pattern Recognition (CVPR)*. IEEE, New Orleans, LA, USA, 15617–15629. [doi:10.1109/CVPR52688.2022.01519](https://doi.org/10.1109/CVPR52688.2022.01519)
- [81] Vincent Sitzmann, Julien Martel, Alexander Bergman, David Lindell, and Gordon Wetzstein. 2020. Implicit neural representations with periodic activation functions. *Advances in neural information processing systems* 33 (2020), 7462–7473.
- [82] Lorenzo Solari, Andrea Ciampalini, Federico Raspini, Silvia Bianchini, Ivana Zinno, Manuela Bonano, Michele Manunta, Sandro Moretti, and Nicola Casagli. 2017. Combined Use of C- and X-Band SAR Data for Subsidence Monitoring in an Urban Area. *Geosciences* 7, 2 (June 2017), 21. [doi:10.3390/geosciences7020021](https://doi.org/10.3390/geosciences7020021) Number: 2 Publisher: Multidisciplinary Digital Publishing Institute.
- [83] Francois Spoto, Omar Sy, Paolo Laberinti, Philippe Martimort, Valerie Fernandez, Olivier Colin, Bianca Hoersch, and Aime Meygret. 2012. Overview Of Sentinel-2. In *2012 IEEE International Geoscience and Remote Sensing Symposium*. 1707–1710. [doi:10.1109/IGARSS.2012.6351195](https://doi.org/10.1109/IGARSS.2012.6351195) ISSN: 2153-7003.
- [84] Gencer Sumbul, Marcela Charfuelan, Begüm Demir, and Volker Markl. 2019. Bigearthnet: A Large-Scale Benchmark Archive for Remote Sensing Image Understanding. In *IGARSS 2019 - 2019 IEEE International Geoscience and Remote Sensing Symposium*. 5901–5904. [doi:10.1109/IGARSS.2019.8900532](https://doi.org/10.1109/IGARSS.2019.8900532) ISSN: 2153-7003.
- [85] Xian Sun, Peijin Wang, Wanxuan Lu, Zicong Zhu, Xiaonan Lu, Qibin He, Junxi Li, Xuee Rong, Zhuojun Yang, Hao Chang, Qinglin He, Guang Yang, Ruiping Wang, Jiwen Lu, and Kun Fu. 2023. RingMo: A Remote Sensing Foundation Model With Masked Image Modeling. *IEEE Transactions on Geoscience and Remote Sensing* 61 (2023), 1–22. [doi:10.1109/TGRS.2023.3194732](https://doi.org/10.1109/TGRS.2023.3194732) Conference Name: IEEE Transactions on Geoscience and Remote Sensing.

- [86] K. Tachi, K. Arai, and Y. Sato. 1989. Advanced microwave scanning radiometer (AMSR): requirements and preliminary design study. *IEEE Transactions on Geoscience and Remote Sensing* 27, 2 (March 1989), 177–183. doi:10.1109/36.20296 Conference Name: IEEE Transactions on Geoscience and Remote Sensing.
- [87] Matthew Tancik, Pratul P. Srinivasan, Ben Mildenhall, Sara Fridovich-Keil, Nithin Raghavan, Utkarsh Singhal, Ravi Ramamoorthi, Jonathan T. Barron, and Ren Ng. 2020. Fourier Features Let Networks Learn High Frequency Functions in Low Dimensional Domains. <http://arxiv.org/abs/2006.10739> arXiv:2006.10739 [cs].
- [88] Alan A. Thompson*. 2015. Overview of the RADARSAT Constellation Mission. *Canadian Journal of Remote Sensing* 41, 5 (Sept. 2015), 401–407. doi:10.1080/07038992.2015.1104633 Publisher: Canadian Aeronautics and Space Institute _eprint: <https://doi.org/10.1080/07038992.2015.1104633>.
- [89] Ramon Torres, Paul Snoei, Dirk Geudtner, David Bibby, Malcolm Davidson, Evert Attema, Pierre Potin, Björn Rommen, Nicolas Floury, Mike Brown, Ignacio Navas Traver, Patrick Deghaye, Berthyl Duesmann, Betlem Rosich, Nuno Miranda, Claudio Bruno, Michelangelo L’Abbate, Renato Croci, Andrea Pietropaolo, Markus Huchler, and Friedhelm Rostan. 2012. GMES Sentinel-1 mission. *Remote Sensing of Environment* 120 (May 2012), 9–24. doi:10.1016/j.rse.2011.05.028
- [90] Gabriel Tseng, Ruben Cartuyvels, Ivan Zvonkov, Mirali Purohit, David Rolnick, and Hannah Kerner. 2024. Lightweight, Pre-trained Transformers for Remote Sensing Timeseries. doi:10.48550/arXiv.2304.14065 arXiv:2304.14065 [cs].
- [91] Arsenios Tsokas, Maciej Rysz, Panos M. Pardalos, and Kathleen Dipple. 2022. SAR data applications in earth observation: An overview. *Expert Systems with Applications* 205 (Nov. 2022), 117342. doi:10.1016/j.eswa.2022.117342
- [92] Ashish Vaswani, Noam Shazeer, Niki Parmar, Jakob Uszkoreit, Llion Jones, Aidan N. Gomez, Lukasz Kaiser, and Illia Polosukhin. 2023. Attention Is All You Need. doi:10.48550/arXiv.1706.03762 arXiv:1706.03762 [cs].
- [93] Di Wang, Qiming Zhang, Yufei Xu, Jing Zhang, Bo Du, Dacheng Tao, and Liangpei Zhang. 2023. Advancing Plain Vision Transformer Toward Remote Sensing Foundation Model. *IEEE Transactions on Geoscience and Remote Sensing* 61 (2023), 1–15. doi:10.1109/TGRS.2022.3222818 Conference Name: IEEE Transactions on Geoscience and Remote Sensing.
- [94] Qunming Wang, Wenzhong Shi, Zhongbin Li, and Peter M. Atkinson. 2016. Fusion of Sentinel-2 images. *Remote Sensing of Environment* 187 (Dec. 2016), 241–252. doi:10.1016/j.rse.2016.10.030
- [95] Yi Wang, Conrad M. Albrecht, Nassim Ait Ali Braham, Lichao Mou, and Xiao Xiang Zhu. 2022. Self-Supervised Learning in Remote Sensing: A review. *IEEE Geoscience and Remote Sensing Magazine* 10, 4 (Dec. 2022), 213–247. doi:10.1109/MGRS.2022.3198244 Conference Name: IEEE Geoscience and Remote Sensing Magazine.
- [96] Yi Wang, Hugo Hernández Hernández, Conrad M. Albrecht, and Xiao Xiang Zhu. 2023. Feature Guided Masked Autoencoder for Self-supervised Learning in Remote Sensing. doi:10.48550/arXiv.2310.18653 arXiv:2310.18653 [cs].
- [97] Rolf Werninghaus and Stefan Buckreuss. 2010. The TerraSAR-X Mission and System Design. *IEEE Transactions on Geoscience and Remote Sensing* 48, 2 (Feb. 2010), 606–614. doi:10.1109/TGRS.2009.2031062
- [98] Zhiyu Wu, Xiaokang Chen, Zizheng Pan, Xingchao Liu, Wen Liu, Damai Dai, Huazuo Gao, Yiyang Ma, Chengyue Wu, Bingxuan Wang, Zhenda Xie, Yu Wu, Kai Hu, Jiawei Wang, Yaofeng Sun, Yukun Li, Yishi Piao, Kang Guan, Aixin Liu, Xin Xie, Yuxiang You, Kai Dong, Xingkai Yu, Haowei Zhang, Liang Zhao, Yisong Wang, and Chong Ruan. 2024. DeepSeek-VL2: Mixture-of-Experts Vision-Language Models for Advanced Multimodal Understanding. doi:10.48550/arXiv.2412.10302 arXiv:2412.10302 [cs].
- [99] Michael A. Wulder, David P. Roy, Volker C. Radeloff, Thomas R. Loveland, Martha C. Anderson, David M. Johnson, Sean Healey, Zhe Zhu, Theodore A. Scambos, Nima Pahlevan, Matthew Hansen, Noel Gorelick, Christopher J. Crawford, Jeffrey G. Masek, Txomin Hermosilla, Joanne C. White, Alan S. Belward, Crystal Schaaf, Curtis E. Woodcock, Justin L. Huntington, Leo Lymburner, Patrick Hostert, Feng Gao, Alexei Lyapustin, Jean-Francois Pekel, Peter Strobl, and Bruce D. Cook. 2022. Fifty years of Landsat science and impacts. *Remote Sensing of Environment* 280 (Oct. 2022), 113195. doi:10.1016/j.rse.2022.113195
- [100] Zhitong Xiong, Yi Wang, Fahong Zhang, Adam J. Stewart, Joëlle Hanna, Damian Borth, Ioannis Papoutsis, Bertrand Le Saux, Gustau Camps-Valls, and Xiao Xiang Zhu. 2024. Neural Plasticity-Inspired Multimodal Foundation Model for Earth Observation. doi:10.48550/arXiv.2403.15356 arXiv:2403.15356 [cs].
- [101] Dejie Xu, Peihao Wang, Yifan Jiang, Zhiwen Fan, and Zhangyang Wang. 2022. Signal Processing for Implicit Neural Representations. *Advances in Neural Information Processing Systems* 35 (Dec. 2022), 13404–13418. https://proceedings.neurips.cc/paper_files/paper/2022/hash/575c450013d0e99e4b0ecf82bd1afaa4-Abstract-Conference.html
- [102] Qiming Zhang, Yufei Xu, Jing Zhang, and Dacheng Tao. 2022. VSA: Learning Varied-Size Window Attention in Vision Transformers. In *Computer Vision – ECCV 2022*, Shai Avidan, Gabriel Brostow, Moustapha Cissé, Giovanni Maria Farinella, and Tal Hassner (Eds.). Springer Nature Switzerland, Cham, 466–483. doi:10.1007/978-3-031-19806-9_27
- [103] Weijia Zhang, Jindong Han, Zhao Xu, Hang Ni, Hao Liu, and Hui Xiong. 2024. Urban Foundation Models: A Survey. In *Proceedings of the 30th ACM SIGKDD Conference on Knowledge Discovery and Data Mining (KDD ’24)*. Association for Computing Machinery, New York, NY, USA, 6633–6643. doi:10.1145/3637528.3671453
- [104] Lijun Zhao, Ping Tang, and Lianzhi Huo. 2016. Feature significance-based multibag-of-visual-words model for remote sensing image scene classification. *Journal of Applied Remote Sensing* 10, 3 (July 2016), 035004. doi:10.1117/1.JRS.10.035004 Publisher: SPIE.
- [105] Yue Zhou, Litong Feng, Yiping Ke, Xue Jiang, Junchi Yan, Xue Yang, and Wayne Zhang. 2024. Towards Vision-Language Geo-Foundation Model: A Survey. doi:10.48550/arXiv.2406.09385 arXiv:2406.09385 [cs].

- [106] Xiao Xiang Zhu, Jingliang Hu, Chunping Qiu, Yilei Shi, Jian Kang, Lichao Mou, Hossein Bagheri, Matthias Häberle, Yuansheng Hua, Rong Huang, Lloyd Hughes, Hao Li, Yao Sun, Guichen Zhang, Shiyao Han, Michael Schmitt, and Yuanyuan Wang. 2019. SoSat LCZ42: A Benchmark Dataset for Global Local Climate Zones Classification. doi:10.48550/arXiv.1912.12171 arXiv:1912.12171 [cs].
- [107] Xiao Xiang Zhu, Zhitong Xiong, Yi Wang, Adam J. Stewart, Konrad Heidler, Yuanyuan Wang, Zhenghang Yuan, Thomas Dujardin, Qingsong Xu, and Yilei Shi. 2024. On the Foundations of Earth and Climate Foundation Models. <http://arxiv.org/abs/2405.04285> arXiv:2405.04285 [cs, eess].

Received 16 April 2025